

QATAR UNIVERSITY

COLLEGE OF ENGINEERING

A TWELVE-PULSE LOAD COMMUTATED CONVERTER DRIVE SYSTEM WITH
VSI FOR STARTING UP AND ACTIVE POWER FILTERING IN AN LNG
APPLICATION

BY

FAISAL IFTIKHAR KHAN

A Thesis Submitted to the Faculty of the
College of Engineering
in Partial Fulfillment
of the Requirements
for the Degree of
Masters of Science in
Electrical Engineering

June 2016

© 2016 Faisal Iftikhar Khan. All Rights Reserved.

COMMITTEE PAGE

The members of the Committee approve the thesis of FAISAL IFTIKHAR KHAN defended on 18/05/2016.

Dr. Ahmed Massoud

Thesis Supervisor

Dr. Lazhar Ben Brahim

Committee Member

Dr. Adel Gastli

Committee Member

Dr. Josep M. Guerrero (External Examiner)

Committee Member

Approved:

Dr. Khalid Al-Khalifa, Dean, College of Engineering

ABSTRACT

Variable Frequency Drives (VFDs) are an integral component of the industry in today's age. VFDs provide a great range of control for electrical machines, and can be integrated in a variety of applications to meet the desired objectives of operation with improved reliability and efficiency.

This thesis presents the Load-Commutated Converter (LCC) drive, which belongs to the Current Source Converter (CSC) based drive system family. Such drives are widely used in high power applications, due to power handling capabilities and the maturity of the drive system. The application under study is that of a helper/starter motor for a turbine compressor in a Liquefied Natural Gas (LNG) plant. Primarily, the thesis presents real-life scenarios of drive system operation such as constant/variable speed operation at constant/varying torque. The respective controllers for the LCC drive are presented alongside their results.

In addition to simulating the drive system in this LNG application, current harmonic mitigation measures are presented in this study. The typical converter topology presented in this thesis is the 12-pulse type, however comparisons with different topologies (6, 18, and 24-pulse) have also been presented.

Finally, a dual-purpose external Voltage Source Inverter (VSI) is used both as a starter and an Active Power Filter (APF), therefore addressing the issues of drive/load induced harmonics and LCC starting. As a conclusion, a controlled LCC drive model is simulated in SIMULINK to emulate the drive operation in actual plant conditions. The controlled

drive is further studied for the presence of harmonics and their subsequent mitigation, by using passive as well as active power filters. The results obtained present the adequacy of the control system as well as the efficacy of the filters used for harmonics mitigation.

Future work revolves around improving the efficiency of the APF, and the drive control system to be more robust and reliable. The system can further be investigated for enhancements as per operational requirements.

TABLE OF CONTENTS

LIST OF FIGURES	ix
LIST OF TABLES.....	xiii
ACKNOWLEDGEMENTS.....	xv
CHAPTER 1 . INTRODUCTION	1
1.1 BACKGROUND.....	1
1.2 PROBLEM STATEMENT AND THESIS OBJECTIVES.....	4
1.3 DRIVE SYSTEM	6
1.3.1 ADVANAGES OF ELECTRIC DRIVE SYSTEM	8
1.3.2 ADVANTAGES OF LCC DRIVES.....	10
1.3.3 DISADVANTAGES OF LCC DRIVES	10
CHAPTER 2 . LITERATURE REVIEW.....	13
2.1 INTRODUCTION.....	13
2.2 LINE COMMUTATED CONVERTERS (LCC).....	14
2.2.1 6-PULSE.....	14
2.2.2 12-PULSE.....	15
2.3 SELF COMMUTATED CONVERTERS	16
2.3.1 VOLTAGE SOURCE CONVERTER (VSC).....	17
2.3.2 CURRENT SOURCE CONVERTER.....	22
2.3.3 COMPARISON BETWEEN LCC AND VSC.....	23

2.4 LOAD COMMUTATED RECTIFIER (LCR).....	24
2.4.1 MULTI-PULSE SCR LOAD COMMUTATED CONVERTER (LCC)	25
2.4.2 THYRISTOR OUTPUT VOLTAGE AND CURRENT	27
2.5 MUTI-WINDING TRANSFORMER IN 12-PULSE TOPOLOGY	30
2.6 PULSE NUMBER.....	33
2.7 INVERTER	35
2.8 LCC STARTING TECHNIQUES	36
CHAPTER 3 . LCC DRIVE CONTROL AND 6-PHASE MOTOR MODELLING	38
3.1 OPERATION OF LCC.....	38
3.2 LCC DRIVE TOPOLOGIES	40
3.3 OPERATION AND CONTROL APPROACH.....	41
3.4 SIX PHASE MOTOR MODELLING	43
3.5.1 SIX-PHASE SYNCHRONOUS MOTOR MODEL IN SYNCHRONOUSLY ROTATING REFERENCE FRAME.....	46
3.5.2 SIMULATION CONSIDERATIONS.....	48
CHAPTER 4 . SIMULATION RESULTS	50
4. 1 RECTIFIER STAGE.....	50
4.2 INVERTER	54
4.3 SPEED CONTROL	58
4.3.1 LCC OPERATION WITH CONSTANT SPEED VARIABLE TORQUE	61
CHAPTER 5 . MITIGATION OF HARMONICS	65

5.1 HARMONICS	65
5.2 POWER FACTOR	66
5.3 6-pulse topology	69
5.4 12-PULSE TOPOLOGY	70
5.5 12-PULSE TOPOLOGY WITH PASSIVE FILTER.....	71
5.6 24-PULSE TOPOLOGY	74
CHAPTER 6 . ACTIVE POWER FILTER	76
6.1 Introduction	76
6.1.1 ACTIVE FILTER OVER PASSIVE FILTER	76
6.1.2 CSI APF vs VSI APF	79
6.1.3 SHUNT APF VS SERIES APF	79
6.2 HARMONIC CURRENT EXTRACTION	81
6.3 APF FOR VAR COMPENSATION AND HARMONICS MITIGATION.....	88
6.4 DUAL FUNCTIONALITY OF THE VSI	92
CHAPTER 7 . CONCLUSION AND FUTURE WORK.....	94
REFERENCES	97
APPENDIX A: LCC TOPOLOGIES	110
APPENDIX B: THYRISTOR FIRING	111
APPENDIX C: LCC SIMULATION BLOCK.....	112
General Schematic.....	112

LCC CONTROL 113

LIST OF FIGURES

FIGURE 1.1: VFD GENERAL SCHEMATIC	6
FIGURE 1.2: SIMPLIFIED LNG PROCESS	7
FIGURE 1.3: GENERAL PROCESS SCHEMATIC	9
FIGURE 2.1: HIGH POWER MEDIUM VOLTAGE CONVERTER CLASSIFICATION.....	13
FIGURE 2.2: 6-PULSE LCR	15
FIGURE 2.3: 12-PULSE LCR	16
FIGURE 2.4: VSC 2-LEVEL CONVERTER (SINGLE PHASE)	17
FIGURE 2.5: DIODE CLAMPED (SINGLE PHASE LEG).....	18
FIGURE 2.6: FLYING CAPACITOR CONVERTER (SINGLE PHASE LEG).....	19
FIGURE 2.7: SINGLE H-BRIDGE CELL	20
FIGURE 2.8: MODULAR MULTI-LEVEL (SINGLE PHASE LEG)	21
FIGURE 2.9: THREE-PHASE CSI	23
FIGURE 2.10: SIX-PULSE RECTIFIER	24
FIGURE 2.11: 2X6 PULSE CONFIGURATION.....	25
FIGURE 2.12: 6 PULSE LOAD COMMUTATED RECTIFIER SWITCHING SEQUENCE	26
FIGURE 2.13: PHASE DISTRIBUTION FOR 6 PULSES.....	29
FIGURE 2.14: PHASE DISTRIBUTION FOR 12 PULSES.....	29
FIGURE 2.15: MULTI-PHASE WINDING	30
FIGURE 2.16: SIMPLE SCHEMATIC WITH SINGLE TRANSFORMER SECONDARY WINDING	31
FIGURE 2.17: CURRENT WAVEFORMS AT THE UTILITY SIDE.....	32
FIGURE 2.18: SPECTRUM OF GRID CURRENT HARMONICS	32

FIGURE 2.19: GRID CURRENTS DUAL TRANSFORMER SECONDARY WINDINGS.....	33
FIGURE 2.20: THD OF GRID CURRENTS.....	33
FIGURE 2.21: RECTIFIED VOLTAGE WITH 6 PULSE CONFIGURATION.....	34
FIGURE 2.22: RECTIFIED VOLTAGE WITH 12 PULSE CONFIGURATION.....	34
FIGURE 2.23: CSI STRUCTURE.....	35
FIGURE 2.24: VSI STRUCTURE.....	35
FIGURE 3.1: LCC DRIVE TOPOLOGY 2.....	40
FIGURE 3.2: GENERAL LCC CONTROL MECHANISM.....	42
FIGURE 3.3: 6-PHASE MOTOR: (A) SYMMETRICAL AND (B) ASYMMETRICAL.....	44
FIGURE 3.4: SIX PHASE MOTOR ILLUSTRATION.....	46
FIGURE 4.1: 12 PULSE RECTIFIER CONFIGURATION WITH CURRENT CONTROL.....	51
FIGURE 4.2: RECTIFIED VOLTAGE AT 0 DEGREES FOR 6-PULSE RECTIFIER.....	52
FIGURE 4.3: RECTIFIED VOLTAGE AT 30 DEGREES FOR 6-PULSE RECTIFIER.....	52
FIGURE 4.4: RECTIFIED VOLTAGE AT 60 DEGREES FOR 6-PULSE RECTIFIER.....	52
FIGURE 4.5: RECTIFIED VOLTAGE AT 0 DEGREES FOR 12-PULSE RECTIFIER.....	53
FIGURE 4.6: RECTIFIED VOLTAGE AT 180 DEGREES FOR 12-PULSE RECTIFIER.....	53
FIGURE 4.7: CURRENT CONTROL IMPLEMENTED IN RECTIFIER BLOCK.....	54
FIGURE 4.8: 12-PULSE INVERTER SCHEMATIC.....	55
FIGURE 4.9: LCI INPUT VOLTAGE WAVEFORM.....	56
FIGURE 10: MOTOR SPEED.....	57
FIGURE 4.11: CONTROL ANGLE FEEDBACK BLOCK DIAGRAM.....	58
FIGURE 4.12: SPEED RESPONSE WITH CONTROLLER.....	59
FIGURE 4.13: SCHEMATIC FOR BACK-TO-BACK CONVERTER CONFIGURATION.....	60
FIGURE 4.14: SPEED RESPONSE WITH MODIFIED CONTROLLER GAINS.....	61

FIGURE 4.15: IMPROVED ELECTROMAGNETIC TORQUE RESPONSE OF MOTOR.....	62
FIGURE 4.16: SPEED RESPONSE WITH INCREMENTAL MECHANICAL TORQUE	63
FIGURE 4.17: STATOR CURRENTS AT CONSTANT SPEED OPERATION.....	63
FIGURE 5.1: GRID CURRENT WITH 6-PULSE TOPOLOGY.....	69
FIGURE 5.2: THD WITH 6-PULSE SYSTEM.....	69
FIGURE 5.3: GRID CURRENT WITH 12-PULSE TOPOLOGY.....	70
FIGURE 5.4: GRID CURRENT THD WITH 12-PULSE TOPOLOGY	71
FIGURE 5.5: GRID CURRENT WITH 12-PULSE TOPOLOGY WITH INPUT FILTER.....	72
FIGURE 5.6: THD WITH 12-PULSE TOPOLOGY WITH PASSIVE FILTER.....	72
FIGURE 5.7: PASSIVE FILTER CONFIGURATION.....	73
FIGURE 5.8: GRID CURRENT WITH 24-PULSE TOPOLOGY.....	74
FIGURE 5.9: THD WITH 24-PULSE TOPOLOGY	74
FIGURE 6.1: ACTIVE POWER FILTER SCHEMATIC	78
FIGURE 6.2: APF CONTROL SCHEMATIC	83
FIGURE 6.3: DC VOLTAGE ACROSS CAPACITOR OF APF INVERTER.....	85
FIGURE 6.4: ID CURRENT COMPONENT.....	85
FIGURE 6.5: IQ CURRENT COMPONENT	86
FIGURE 6.6: GRID CURRENT WITHOUT APF	86
FIGURE 6.7: THD OF CURRENT WITHOUT APF.....	87
FIGURE 6.8: GRID CURRENT WITH TUNED APF	87
FIGURE 6.9: THD OF CURRENT WITH APF	87
FIGURE 6.10: PI CURRENT CONTROL OF APF	88
FIGURE 6.11: LOAD CURRENT	89
FIGURE 6.12: HARMONIC CONTENT IN THE LOAD CURRENT	89

FIGURE 6.13: FILTER CURRENT	90
FIGURE 6.14: HARMONIC SPECTRUM.....	90
FIGURE 6.15: SUPPLY VOLTAGE ALONGSIDE CURRENT	91
FIGURE 6.16: FILTERED SUPPLY CURRENT	91
FIGURE 6.17: FREQUENCY SPECTRUM OF SUPPLY CURRENT	91
FIGURE 6.18: DUAL FUNCTION VSI.....	93

LIST OF TABLES

TABLE 1.1: HARMONIC MITIGATION APPROACHES	11
TABLE 4.1: MOTOR PARAMETERS	57
TABLE 4.2: CONTROLLER GAINS	59
TABLE 5.1: THD COMPARISON WITH DIFFERENT TOPOLOGIES	75
TABLE 6.1: CURRENT SOURCE AND VOLTAGE SOURCE APF	79
TABLE 6.2: SHUNT AND SERIES APF COMPARISON	80
TABLE 6.3: APF TESTING PARAMETERS.....	84

LIST OF ACRONYMS

LNG	LIQUIFIED NATURAL GAS
VFD	VARIABLE FREQUENCY DRIVE
LCC	LOAD COMMUTATED CONVERTER
LCR	LOAD COMMUTATED RECTIFIER
LCI	LOAD COMMUTATED INVERTER
SCC	SELF COMMUTATED CONVERTER
SCR	SILICON CONTROLLED RECTIFIER
CSI	CURRENT SOURCE INVERTER
VSI	VOLTAGE SOURCE INVERTER
THD	TOTAL HARMONIC DISTORTION
PF	POWER FACTOR
VAR	VOLT-AMPERE REACTIVE
PMSM	PERMANENT MAGNET SYNCHRONOUS MOTOR
APF	ACTIVE POWER FILTER

ACKNOWLEDGEMENTS

I would like to acknowledge my family, friends and my supervisor for continually supporting me during the course of this thesis completion. I had to work alongside my work outside and therefore time management was an issue and without Dr. Ahmed Massoud's positive attitude this would not have been possible.

CHAPTER 1 . INTRODUCTION

This thesis addresses a Load Commuted Converter (LCC) drive for synchronous motors in high power applications in the field of Liquefied Natural Gas (LNG) plants. The building blocks of the drive system, namely the rectifier (Load Commutated Rectifier (LCR)), inverter (Load Commutated Inverter (LCI)) and the control system are separately discussed, simulated and relevant case studies are presented throughout the thesis, followed by LCI starting and filtering techniques in order to improve the performance of the drive while preventing current harmonics to be injected to the grid.

Qatar has roughly 14% of the known global gas reserves, making it the third most abundant country [1] after Russia and Iran. QatarGas and RasGas (both owned by Qatar Petroleum) are jointly producing approximately 77 million tonnes of LNG per annum.

1.1 BACKGROUND

SCR is a semi-controlled semiconductor device used in high power conversion [47] and control in industrial applications. Due to the high power (up to 12 kV and 5 KA ratings) capabilities of the modern SCRs, they have become quite a reputable choice of switching devices in such high power fields.

The first member of the thyristor family is the SCR. Compared to transistors; the thyristors have less on-state conduction losses and greater power handling capabilities

[48]. In addition to full controllability, transistors however have a higher switching frequency capability.

In high power applications, such as helper motor drives for LNG compressors, switching elements, such as thyristors are used due to their power handling capabilities. With SCR used in LCC, active power conversion from full negative to full positive rating is possible, however inductive reactive power is absorbed by the system [48-49]. The DC current in this conversion is controlled from 0 to rated value, however the DC voltage can be controlled between \pm rated value.

The switching capabilities of thyristors do introduce a lot of harmonics in the current that could be fed back to the grid or utility provider. Effect of such harmonics [2-4] in the system lead to transformer losses, create metering conflicts, and also cause disturbances to the other connected equipment to the grid.

In order to meet the specifications of the IEEE standards [49] for current harmonic distortions, different methods can be implemented such as:

- a. Using inductors [50] as a passive filter or with combination of a capacitor, however the latter is not a desired technique due to the possibility of resonance occurrence at specific frequencies.
- b. Using multi-phase [51] rectifiers/inverters as they cancel out the harmonics from the line-side converter currents.
- c. Multi-winding transformers [52-54] that are used to feed the multi-phase rectifiers also introduce a phase shift of 30° at the secondary side of the transformer that cancel out the 5th and 7th harmonics from the line side currents. The effect of these

phase-shifting transformers is illustrated in the following sections in a detailed manner.

In simple terms, the thyristor looks like a diode with an added gate signal. This gate signal is responsible for controlling the thyristor. As seen from the current-voltage characteristics, when forward biased, the thyristor continues to conduct even if the gate signal is removed. Turning the thyristors off would require commutation techniques, which are discussed further ahead.

Thyristors have three states:

- a. Reverse blocking state: Voltage is applied in the direction that would be blocked by a diode.
- b. Forward blocking state: Voltage is applied in the direction that would cause a diode to conduct, but the thyristor has not yet been triggered into conduction
- c. Forward conducting state: The thyristor can be triggered into conduction by applying a gate current and remains in conducting state until the forward current drops below a threshold value known as the holding current.

Once the thyristor begins to conduct, the gate signal can be removed and it continues to conduct as a diode. It is to be noted that the thyristor cannot be turned off by the gate signal. The thyristor turns off when the anode current goes to negative polarity. This enables the gate signal to turn on the thyristor if it enters the forward blocking mode. At reverse bias condition, below the reverse breakdown voltage, a very small amount of leakage current passes through the thyristor. Usually, the forward and reverse blocking voltage ratings are the same. The gate signals of the thyristors are switched on and off in

a sequence that enable the output to be maintained as a DC. The angle to be controlled is also known as the firing angle.

Firing angle is the phase angle of the voltage at which the SCR is turned on, which is done by applying a gate signal to the thyristor. For fully controlled converters, the average DC voltage output remains positive (rectifier mode) until the firing angle, $\alpha \leq 90^\circ$, and goes negative (inverter mode) when $\alpha \geq 90^\circ$.

In order to turn on thyristor, the following two conditions need to be fulfilled:

1. Positive forward voltage (Potential difference between anode and cathode)
2. Positive gate current

However to turn off a thyristor, the current through it has to be zero.

1.2 PROBLEM STATEMENT AND THESIS OBJECTIVES

This thesis emphasizes on a type of variable frequency drive (VFD) that is used alongside a helper/starter motor in an LNG producing company. The primary objective of the thesis is to develop a working model of the LCC drive system in order to enable studying and proposing improvements. The drive system that is being modeled in this thesis is an integral and critical part of the production train that is being referenced, and therefore a study of the system is of a vital importance. The objectives also extend to proposing solutions for the harmonics mitigation and starting methods for the LCC drive.

With all the added advantages of using LCC drives, there are also some problems that arise. Some of those problems are highlighted in this study alongside their control measures for mitigation and improvement in the over-all operation.

1. One of the most critical drawbacks of using an LCC drive is the introduction of current harmonics [2-4] to the utility or the primary power provider. This is dealt with by showing the impact of
 - Multi-winding transformer
 - 12-pulse system over a 6-pulse system
 - Power filter deployment
2. Torque fluctuations at low speeds [5].
3. Start-up methods. Being able to smoothly start [6-9] the drive system is of vital importance and is critical in LCC applications. A start-up technique is proposed alongside the discussion of other available starting methods.
4. Over-voltage and over-current [10] on the drive end, causing troubles such as diode failures (rotating diodes on the rotating transformer of the exciter). Such over-voltage and current instances can be attributed to operational instabilities such as speed and torque fluctuations.
5. Thyristor faults caused by deterioration, over-heating, snubber circuit failures, etc.

The primary problems tackled in this thesis study are the mitigation of current harmonics that are re-injected to the power grid, alongside the external starting for the LCC drive.

1.3 DRIVE SYSTEM

With growing industry and processes, the need for a flexible and robust means of operation is of high significance. VFDs allow the operation to be adjusted in order to optimize the output, reduce operational costs, and increase efficiency [11-12] to a large extent. This thesis emphasizes on LCC drives that fall under the category of Current Source Converter (CSC) drives.

There are different types of drives [13], namely electrical, hydraulic and mechanical, however this thesis targets electrical drives in specific. An electrical drive consists of three main components as shown in Fig. 1.1.

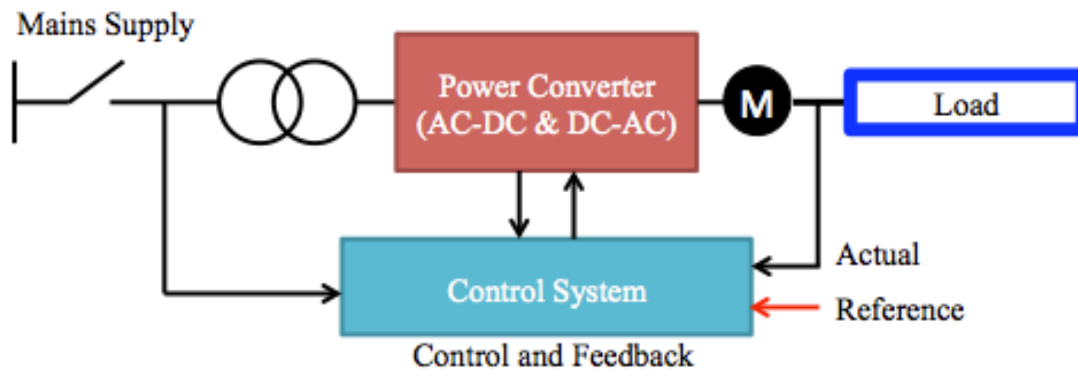


Figure 1.1: VFD general schematic

The applications can vary greatly. This case is dealing with a compressor load, and the electrical drive functions both as a helper and starter for the motor.

In order for LNG to be supplied, it needs to be cooled down to about -162 deg. Celsius that reduces the volume to 1/600th [14-15] of the actual volume, therefore enabling large volumes to be supplied in tankers. For this scale of gas liquefaction, the gas is passed through stages of heat exchangers, where the heat exchange takes place by expansion of the refrigerant. To close the loop, the refrigerant is then re-compressed, cooled and fed back to the heat exchangers. This process can be illustrated in Fig. 1.2 as follows:

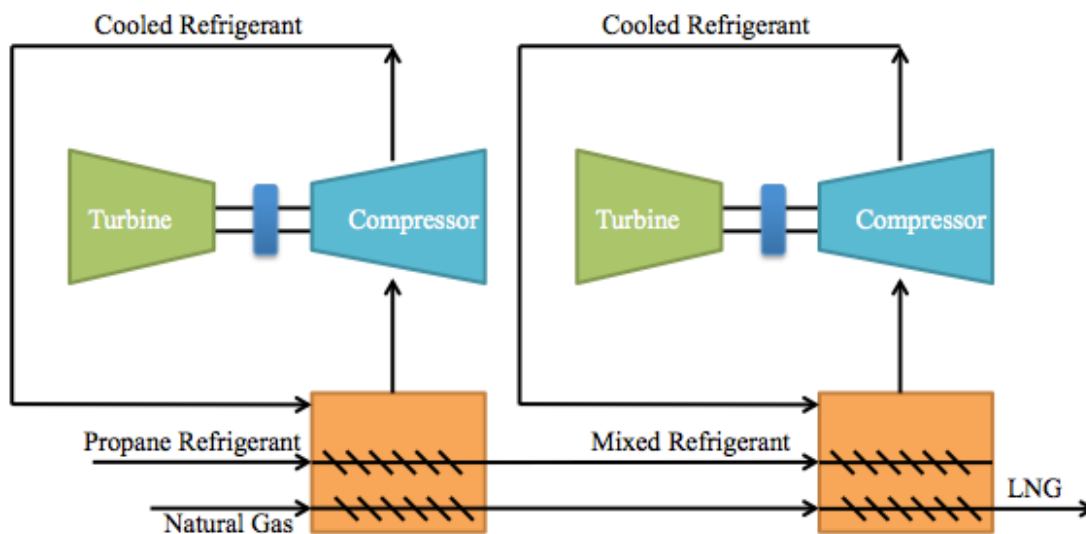


Figure 1.2: Simplified LNG process

In large-scale operations, the compressors are quite large and require turbines to run, however the role of VFDs are quite integral in providing start-ups and steady-state assistance as well.

Typically a separately excited synchronous motor is used in such applications, however the motor being used for simulation in this thesis is a permanent magnet synchronous motor (PMSM).

1.3.1 ADVANAGES OF ELECTRIC DRIVE SYSTEM

There are several advantages of using a drive system in real life electrical applications. Below are some key points that pinpoint the pros of having an electrical drive system:

1. Energy Savings

Energy saving is a direct or indirect benefit of employing electric drive system. Direct energy saving is normally obtained by having loads that require to run at constant speeds; therefore it eliminates the need for physically maintaining speeds by altering the process cycle [13]. The electrical drives alongside speed controllers can be used to allow for constant speed operation with high reliability and efficiency. Examples of such cases are centrifugal pumps or fans that require running at constant speeds.

2. Reduced stress

Using a motor with an electric drive system as opposed to a direct online (DOL) motor has advantages associated to the reduction of mechanical wear and tear of the machine itself. DOL motors also cause high in-rush currents at start up and poor power factors.

Having a controlled start-up can be managed using a VFD and it considerably cuts down motor maintenance, and prolongs the lifetime of the machine.

3. Improved process control

This is an integral factor that introduces a higher efficiency in the process line.

Since the application of compressors in LNG process plants is being referenced to, the general configuration of a turbine, compressor and motors can be demonstrated as follows:

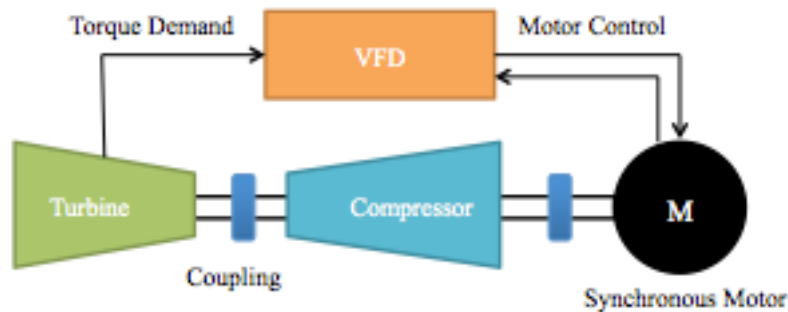


Figure 1.3: General process schematic

As seen in Fig. 1.3, the VFD provides an interface between the turbine and the motor. The torque requirement is input as a reference signal to the VFD control system and the motor is expected to track the necessary reference values accordingly. This process ensures that the compressor maintains the temperature of natural gas at -162 degrees for the gas to remain at liquid state.

Furthermore, the motor can act both as a helper or starter, providing starting, as well as adding extra torque depending on process requirements.

1.3.2 ADVANTAGES OF LCC DRIVES

Some of the main advantages of using an LCC drive system can be summarized as follows [16-18]:

1. Using the LCC drive system in high power applications (above 1000 horsepower) can result in drive efficiencies exceeding 95% at rated power.
2. As compared to the self-commutated converters, the LCC has a simpler design and lesser losses since there is no need for self-controlled switches.
3. LCC drives can also allow for regenerative braking that allows the synchronous motor to be operated as a generator. In this mode, the machine converter works as a rectifier with the generator supplying it with voltage and the line side converter works as an inverter feeding power into the grid.

1.3.3 DISADVANTAGES OF LCC DRIVES

With the numerous benefits, there are also some drawbacks [19] that the LCC drives introduce to the system. Apart from the increased cost of the drive, it's cooling and the extra space requirements are the cons of having this drive system. Moreover the harmonics that are introduced by their deployment are considered disadvantages of the LCC electric drive systems. This is explained as shown below.

1. Harmonics and mitigation

The drive acts as a non-linear load to the utility or the main grid supplying the power. The harmonics [20-22] that are generated, negatively affect the electrical network, and the direct effects can be seen as over-heating of transformers, motors, cables, and generators connected to the same network. Different drive configurations are aimed at reducing these back feeding harmonics by having a multi-pulse inverter configuration (6,12,24 pulse, etc.), or actually having RLC filters implemented alongside the drives. The different methods of mitigating harmonics are summarized in the Table 1.1 [20-22]:

Table 1.1: Harmonic mitigation approaches

Harmonic Mitigation	Pros	Cons
12 pulse Bridge	Elimination of 5 th , 7 th , 17 th , and 19 th harmonics	11 th and 13 th harmonic issues
Passive power filters	Least expensive Applies filtration at PCC	Site checks necessary Cable failures Aging of components Filter tuning
Active power filters	Efficient Higher bandwidth	Expensive

2. Machine side harmonics and consequent impact on motor

The operation of the LCC drive also introduces high current harmonics to the machine side; therefore the motor must be designed specifically to accommodate the harmonic content [23].

CHAPTER 2 . LITERATURE REVIEW

2.1 INTRODUCTION

This section covers the common types of converters used in medium voltage drives for high power application, alongside the one that is presented in this thesis. Since details of other converters are not a major scope of this thesis, only basic information is presented in this section. Fig. 2.1 illustrates the main types of medium voltage drive systems.

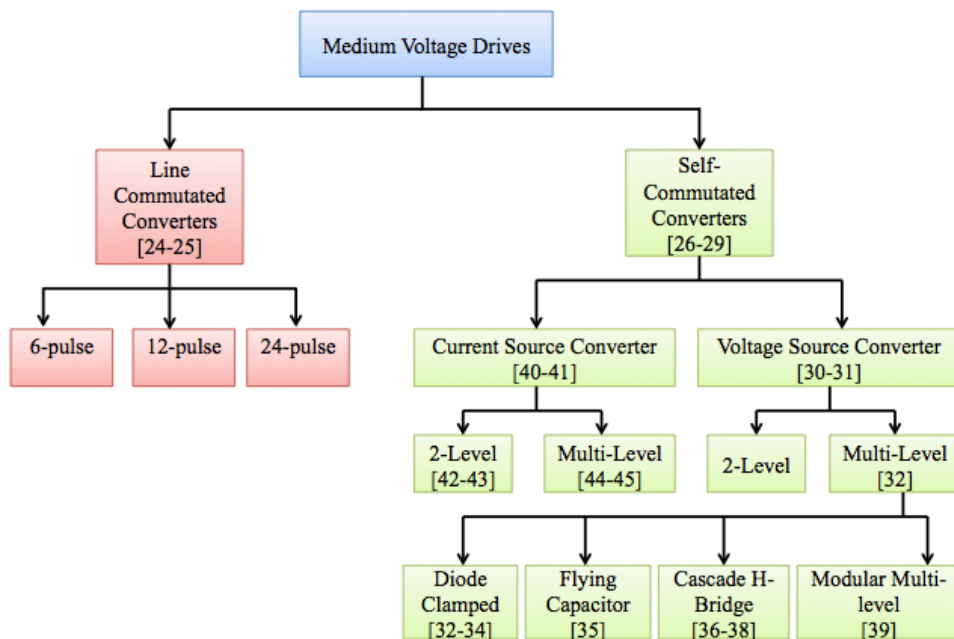


Figure 2.1: High power medium voltage converter classification

2.2 LINE COMMUTATED CONVERTERS (LCC)

Power converters use semiconductor devices for switching purposes to turn on and off repetitively in order for a certain conversion to take place. The LCC employs semi-controlled devices (can be controlled for turn on yet turn off is achieved naturally) as thyristors. When the switch turns off, the current commutates away from the switch. In case of a diode or a thyristor, a reverse bias voltage can cause the commutation to be achieved. Since no external source is required for the commutation to take place [24-25], these types of converters are also known as natural commutated converters. It is important to notice that an LCC can only be used with an AC source since the alternating waveforms are required for commutation purposes.

2.2.1 6-PULSE

The 6-pulse topology is presented below, where thyristors are used as switching elements in a load commutated rectifier (LCR) example. Fig. 2.2 shows the general schematic that is used in this thesis in order to build the 12-pulse topology (primary topology of the LCC model being studied) as shown in the next section.

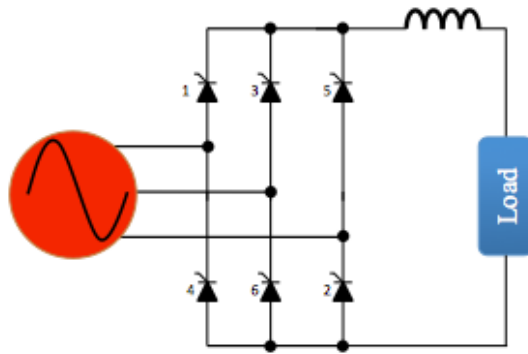


Figure 2.2: 6-pulse LCR

2.2.2 12-PULSE

Building on what is presented in the 6-pulse model, the pulse number increases and also introduces a multi-phase transformer. This is the key topology being presented in this thesis, and a generic schematic is presented in Fig. 2.3.

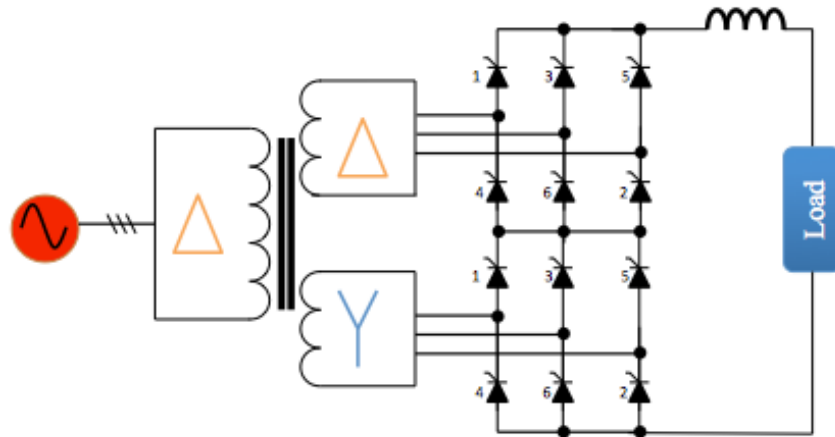


Figure 2.3: 12-pulse LCR

With higher pulse number of the converter alongside the dual secondary windings of the transformer the 12-pulse topology has advantages over the 6-pulse topology as the converter ratings can be increased for high-power applications, as well as harmonic mitigation is effectively done on both grid and load side.

2.3 SELF COMMUTATED CONVERTERS

The commutation in Self-Commutated Converters (SCC) takes place using the components present in the converter itself, and do not rely on external circuit source. SCCs use switching devices that have controlled turn-on and turn-off capabilities, and altering the switching of these devices varies the resulting voltage/current waveforms. It is to be noted that a large stored energy is involved as result of switching at rated current/voltages, therefore presenting the need of costly snubber devices [26-29].

2.3.1 VOLTAGE SOURCE CONVERTER (VSC)

Voltage Source Converters (VSCs) are used quite commonly to transfer power from DC to AC system, or back-to-back AC systems [30-31]. The general structure of a VSC connected to an AC system includes a DC capacitor between the rectifier and the inverter blocks in order to provide a smooth DC voltage. In VSCs, the DC voltage has one polarity and the power flow is determined by the polarity of the DC current polarity.

1. 2 level

The 2-level converters are capable of producing two output phase voltage levels, (namely V_+ and V_-). The circuitry as illustrated in Fig. 2.4 is quite simple however the output AC waveform is high in harmonic content with high dv/dt .

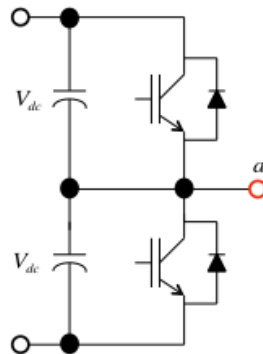


Figure 2.4: VSC 2-level Converter (Single phase)

2. Multilevel

In the multilevel conversion, series-connected switching devices are sequentially switched at the fundamental frequency in order to produce a voltage waveform in steps. As a result, lower order harmonics are reduced as well as reduction in dv/dt ratings [32] of the switching devices is possible.

a. Diode clamped

An n-level diode clamped converter [32-34] produces n-level of voltage per phase and also has n-1 capacitors at the DC bus. As this type has less harmonic content as compared to the 2-level converter type, it does have some disadvantages too. The capacitors suffer from the problem of voltage imbalance. The blocking diodes as shown in Fig. 2.5 also require to be rated for high voltages, and this number increases as the voltage levels increase, introducing more complexity and cost factors.

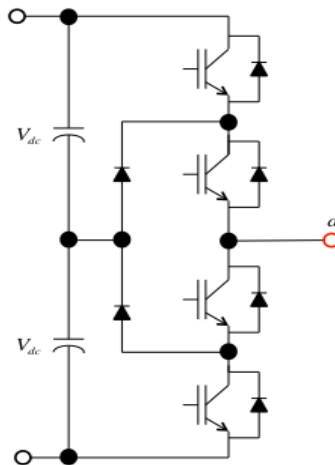


Figure 2.5: Diode Clamped (single phase leg)

b. Flying capacitor

As compared to the diode clamped converter, the flying capacitor type as shown in Fig. 2.6, consists of floating capacitors and this number increases as the intended levels [35] increase. While the disadvantages of such converter include cost and complexity, it does provide ride through capabilities during outages due to the presence of the capacitors. The capacitors however need to be precharged to prevent uncharged capacitors from high voltages at startups.

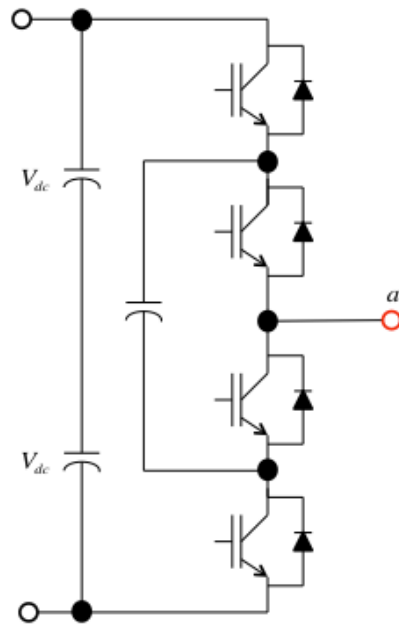


Figure 2.6: Flying Capacitor Converter (Single phase leg)

c. Cascade H bridge

A single branch of an H bridge configuration can produce three voltage levels ($V+$, 0 and $V-$). If this configuration shown in Fig. 2.7 is cascaded in a series format, each staircase step of the voltage output corresponds to an individual H bridge.

For an n -level converter, each phase needs to have $(n-1)/2$ H bridges. In one side, the extra diode and capacitors are removed as shown in the different converters. Yet, this type requires separate DC sources, and this gets difficult at higher voltage [36-38] levels.

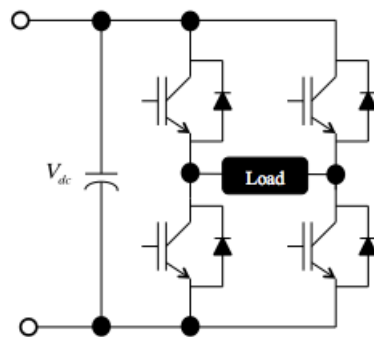


Figure 2.7: Single H-Bridge cell

d. Modular multi-level

This topology as illustrated in Fig. 2.8 uses cells, where each cell consists of a primary switch and an auxiliary switch. Mostly, the output voltage ranges between V^+ and 0, unlike the H bridge configuration where the V^- level is also present.

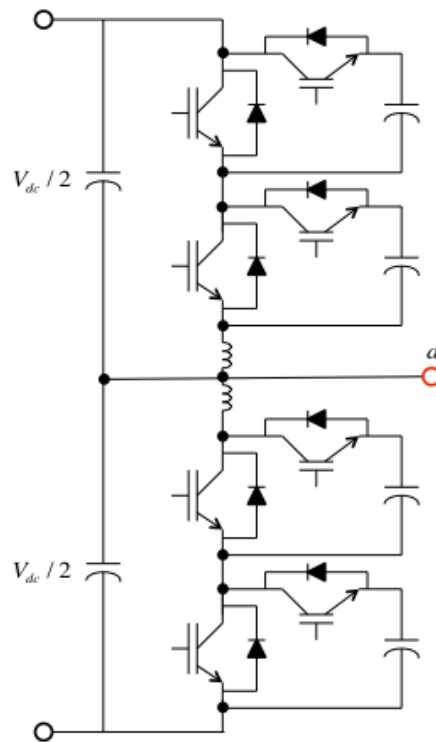


Figure 2.8: Modular multi-level (single phase leg)

At the 0 level, the capacitors either charge or discharge depending on the polarity of the load current and it can cause a voltage imbalance. The capacitor voltages can be controlled by controlling the switching of the different cells at the 0 output voltage level. The inductors help in circulating the current during voltage balancing, and limiting the in-

rush currents. At higher levels of this topology [39], higher voltages can be supported and it can be operational without the use of filters, giving it an edge over other topologies.

2.3.2 CURRENT SOURCE CONVERTER

In a typical Current Source Converter (CSC), the DC current is kept constant using a DC-link reactor, providing a current source at the DC side of the converter. The direction of power flow in a CSC is determined by the polarity of the DC voltage, however the current flow is unidirectional.

CSCs can be divided into categories of PWM-based CSCs, and LCCs, where the former uses symmetrical Gate-Turn Off (GTO) or Integrated Gate Commutated Thyristors (IGCTs) as switching elements, and the latter uses Silicon Controlled Rectifier (SCR) devices. The main drawback [40] of the CSCs lies in their dynamic performance in high power applications, due to the use of large inductors in the DC-link. In high power applications, the use of LCC is preferable due to power handling capabilities, however the power controllability is limited to two-quadrant operation. The increasing power ratings of the self-commutating switches are enabling the CSCs to be used in high power applications. In CSCs, the forced commutation of the switches from rated to zero current requires high electromagnetic energy which is stored in the AC system inductance. Therefore, coupling the CSC to the AC system requires large capacitors.

With LCCs, synchronous motors (SM) are commonly used as the SCRs in the inverter do not have self turn-off capabilities, and leading operation [40] of the SM assists the commutation. Compared to the IGBTs/IGCTs, the thyristors have higher energy

efficiency and low production cost therefore giving the LCCs an edge in high power applications [40].

There are main two types of CSCs, namely the 2 level [42-43] and the multi-level (3-level) [44-45]. A three phase self-commutating CSI is presented in Fig. 2.9.

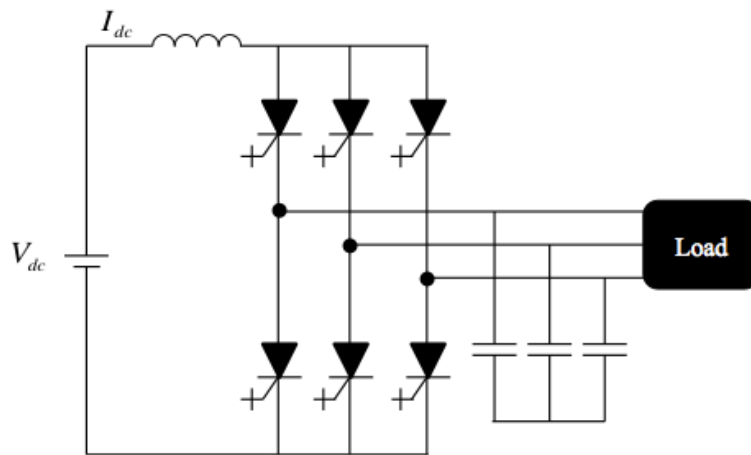


Figure 2.9: Three-phase CSI

2.3.3 COMPARISON BETWEEN LCC AND VSC

As a summary of this section, some key points differentiating the different converters types are presented here. VSC topologies generally work with both induction and synchronous motors. However, LCC drives require motors with low commutation reactance [46]. LCC drives also introduce more current harmonics into the system; therefore, harmonics mitigation measures need to be implemented. Other than being a

reliable and mature technology, the LCC is preferred in high power applications for robustness and the power handling capabilities of the switching elements.

2.4 LOAD COMMUTATED RECTIFIER (LCR)

The rectifier (line-side converter) unit is quite an integral part of this motor drive. This is where the AC input is converted into DC and fed to the machine-side converter. The rectifier unit, as shown in Fig. 2.10, is made up of a thyristor bridge with 6 thyristors in each block, i-e, 2 thyristors per phase. This is used simultaneously with another 6-pulse rectifier block to formulate a 12-pulse rectifier.

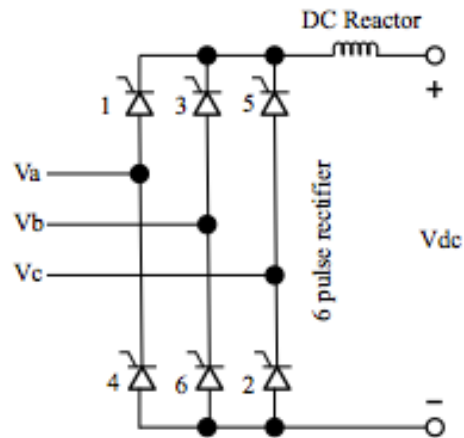


Figure 2.10: Six-pulse rectifier

The basic principle of rectification is where the semiconductor device only conducts so as to keep the flow of current through the load in a positive direction in order to remove the negative cycle of the incoming alternating voltage.

2.4.1 MULTI-PULSE SCR LOAD COMMUTATED CONVERTER (LCC)

As mentioned earlier, the switching phenomenon of the thyristor bridge introduces several harmonics, so the multi-winding transformer [54] is used in conjunction with the multi-pulse rectifier to mitigate the effect of these harmonics. There are 12, 18 and 24 pulse SCR LCCs that are commonly used in the industry.

The application being studied in this thesis is the 12-pulse rectifier unit (2 cascaded 6-pulse rectifiers), as shown in Fig. 2.11. This topology is chosen in order to have a base model to match the one used in the actual case being presented.

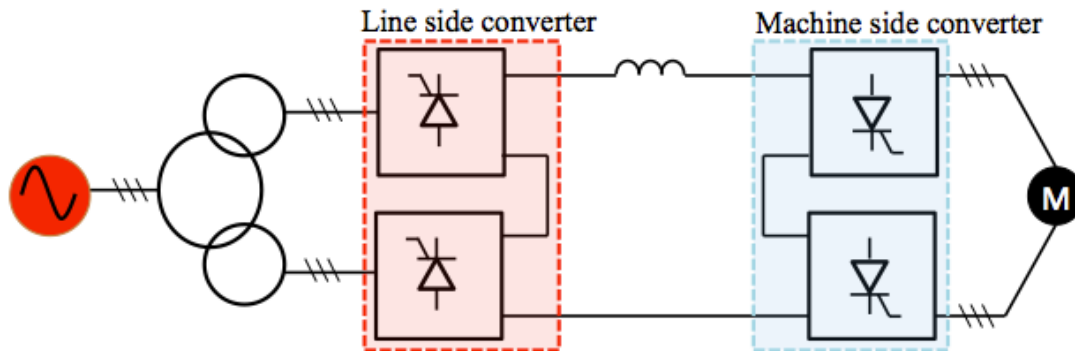


Figure 2.11: 2x6 pulse configuration

This configuration is a modification of having two SCRs in series, where issues of voltage sharing are present. Two SCRs in series are used for high power applications to provide redundancy in case of thyristor failures. Switching in a synchronized manner is also difficult with such configuration. The configuration shown in Fig. 2.11 improves the functionality of the SCRs, whilst reducing grid current harmonics due to the presence of the phase-shifting transformer. During steady-state motoring mode operation, the line side converter functions as a rectifier and the machine side converter as an inverter.

As the pulse number of the rectifiers increases (18 and 24), the secondary windings of the transformer also increase resulting in lower harmonics. Such configurations suit large power applications, however the cost factors have to be weighed against the advantages, for practical implementation.

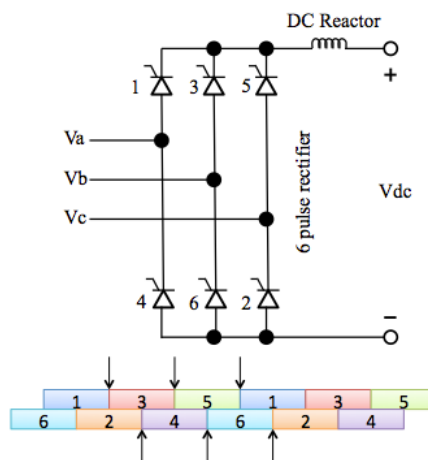


Figure 2.12: 6 pulse load commutated rectifier switching sequence

With the configuration shown in Fig. 2.12, in order for the current to pass through, one SCR from (1,3,5) and one SCR from (4,6,2) should be conducting in turns (during 120 degrees of each supply voltage cycle), to create a path from the positive to the negative pole of the rectifier respectively. The line current of phase a can be expressed as follows:

$$i_a = i_{SCR1} - i_{SCR4} \quad (2.1)$$

The load current (i_L) is the sum of (i_{SCR1} , i_{SCR3} and i_{SCR5}), and is shown as a constant value in case of a highly inductive load presented at the DC side.

As presented in figure 15, the current pulses through SCR 1, 3, and 5 turn on every 120 degrees [55]. The current passing through SCR4 can simply be related to the SCR1 response as it completes the negative cycle of the passing current. I_a is obtained by subtracting SCR4 from SCR1 current sequence.

If the value of the inductive load current (ripple free) is known (I_L), the RMS of the line current ($I_{a,RMS}$) can be obtained from the following expression:

$$I_{a,RMS} = \sqrt{\frac{2}{3}} I_L \quad (2.2)$$

2.4.2 THYRISTOR OUTPUT VOLTAGE AND CURRENT

The output of the thyristors is controlled by the firing angle, α (also known as delay angle). As mentioned previously in the introduction, the greater the value of α , the lower the output voltage and this is illustrated in Figs. 38-40 in later sections. Each supply cycle

has 6 ripples in the output voltage. The average voltage output (load voltage) ($V_{L,average}$) is presented as:

$$V_{L,average} = 3 \frac{1.41}{\pi} V_{LL} \cos\alpha = 1.35 V_{LL} \cos\alpha \quad (2.3)$$

Where V_{LL} is the RMS line voltage. From (2.3) it is seen that as the value of α increases, the voltage across the load decreases in either rectification or inversion modes. So while the value of $\alpha < 90^\circ$, the voltage is positive, i-e being transferred from the source to the load, hence the converter is called to be operating in the rectifier mode. However, if $\alpha > 90^\circ$, energy is being transferred from the load to the source, and the converter is operating in the inverter mode. Theoretically, the value of α ranges from 0 to π radians, however in practice this range can be assumed to be between 10° and 170° . The ideal range of (0- π rad) is only true for the case when source impedance is assumed 0 (infinite short circuit level). Therefore as the source impedance [56] increases (weak power system), the range of α shrinks.

The source impedance of actual AC systems is seldom zero. Due to this impedance, current commutation between different valves takes a non-zero finite time. This commutation delay is a result of source impedance [56], source voltage and the firing angle. Considering the delay, the rectifier terminal voltage V_d is presented as follows:

$$V_d = \frac{V_{d0}}{2} (\cos\alpha + \cos(\alpha + \mu)) \quad (2.4)$$

Where V_{d0} is the ideal no-load direct voltage, and μ is the commutation delay angle.

Since the commutation delay is not always readily known, another expression is of the following form:

$$V_d = V_{d0} \cos\alpha - \frac{3\omega L_c}{\pi} I_d \quad (2.5)$$

Where, L_c is the source inductance and I_d is the rectifier current.

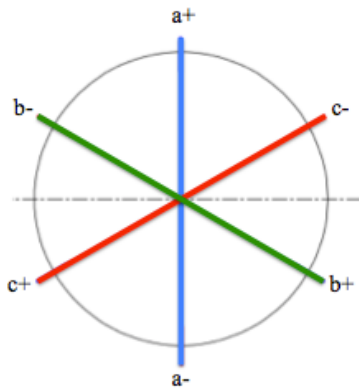


Figure 2.13: Phase distribution for 6 pulses

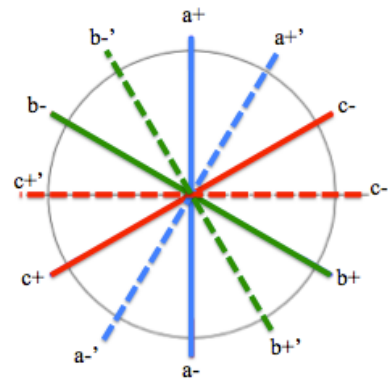


Figure 2.14: Phase distribution for 12 pulses

For the two 3-phase (2x6 pulses) thyristor bridges, there is a commutation every 30 degrees, therefore each fundamental cycle has 12-pulses. These differences between a 6 and a 12-pulse configuration is illustrated in Fig. 2.13 and 2.14.

2.5 MULTI-WINDING TRANSFORMER IN 12-PULSE TOPOLOGY

The reason for introducing the multi-winding transformer here is to have a basic concept before discussing the 12-pulse converter configuration and its significance. As discussed earlier that the LCC drive introduces a harmonics problem that is quite critical, therefore, having multi-winding transformers helps greatly in the reduction of these harmonics [52-54]. The type of transformer used in the relevant application is shown in Fig. 2.15.

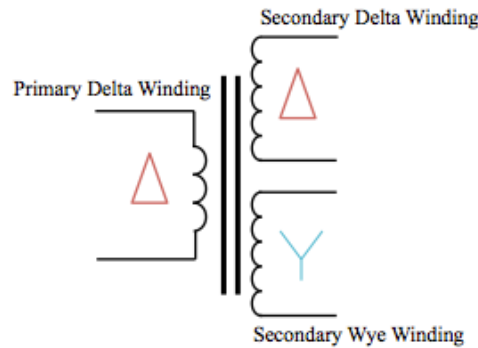


Figure 2.15: Multi-phase winding

Modern electrical distribution systems suffer greatly from harmonic currents due to the presence of non-linear loads such as VFDs as being presented in this thesis. The effects of harmonics range from motor failure and poor power factor to overloaded transformers. A multi-phase or dual-secondary transformer uses the concept of phase shifting to counter the harmonics at the grid side.

The output of the transformer secondary is phase shifted by 30° due to the wye-delta configuration. The primary idea of phase shifting is to displace [52] the harmonic currents until the pairs reach 180° in order to cancel each other out. Positive-sequence currents counter the negative-sequence currents, and the zero-sequence currents act against each other. The triplen harmonic currents are zero-sequence vectors, 5^{th} , 11^{th} , and 17^{th} harmonics are negative-sequence vectors, and 7^{th} , 13^{th} , and 19^{th} harmonics are positive-sequence vectors. The case presented in the thesis, introduces a 30° shift, therefore suppressing 5^{th} and 7^{th} harmonic current pairs.

An illustration of grid currents with and without dual-secondary transformers is presented below, alongside the respective harmonic content.

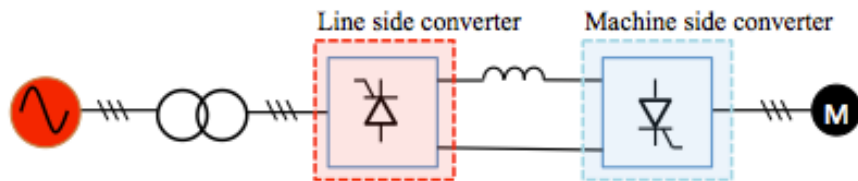


Figure 2.16: Simple schematic with single transformer secondary winding

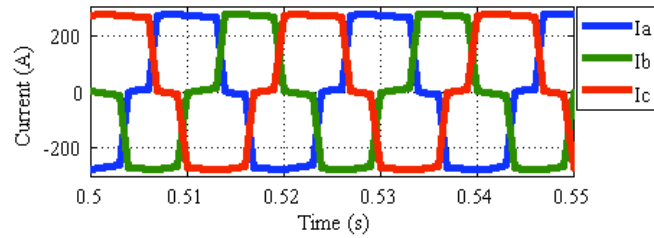


Figure 2.17: Current waveforms at the utility side

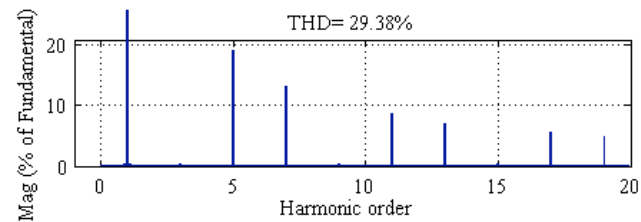


Figure 2.18: Spectrum of grid current harmonics

Grid voltage is stepped down from 33kV to 3.3kV; DC-link inductor of 10 mH, and synchronous motor with 2 poles is used for this simulation to closely match the parameter shown in table 4.1. For the topology presented in Fig. 2.11, the following grid current waveforms are obtained.

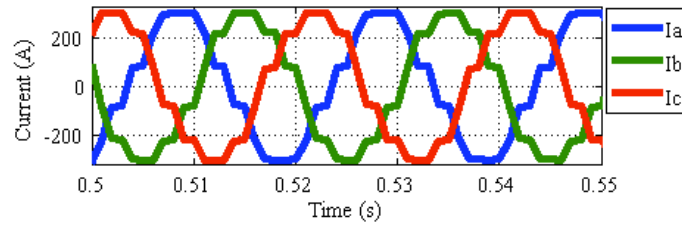


Figure 2.19: Grid currents dual transformer secondary windings

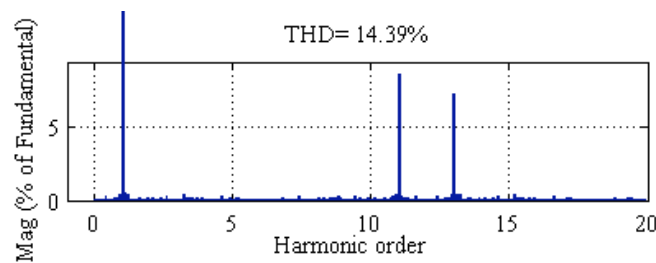


Figure 2.20: THD of grid currents

The significant impact of the dual-secondary transformer is clearly seen in Fig. 22-24, where the THD of current is greatly reduced, and 5th and 7th order harmonics are eliminated.

2.6 PULSE NUMBER

This section illustrates the significance of converter pulse number. The voltage output from a typical six-pulse rectifier is illustrated in Fig. 25, where the base voltage is approximately 1000 V.

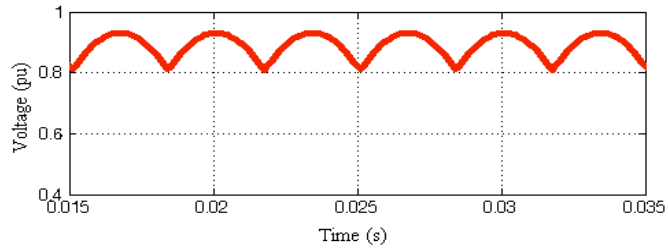


Figure 2.21: Rectified voltage with 6 pulse configuration

However, when a 12-pulse rectifier is used in conjunction with a dual-secondary transformer, the output DC voltage (across a resistive load) is presented in Fig. 2.23:

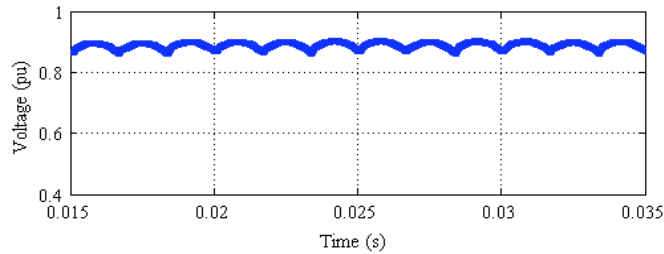


Figure 2.22: Rectified voltage with 12 pulse configuration

As seen from Fig. 2.23 and 2.24, the rectified output voltage from a 12-pulse rectifier fluctuates much less and resembles a DC waveform as opposed to a 6-pulse rectifier.

2.7 INVERTER

The output of the rectifier goes through a DC link that in this case is an inductor. Having an inductor presents the input to the inverter as a current source, therefore making this a current source inverter (CSI). The rectifier block in Fig. 2.24 could be either diode or active front end; however this section is only presenting generic illustrations.

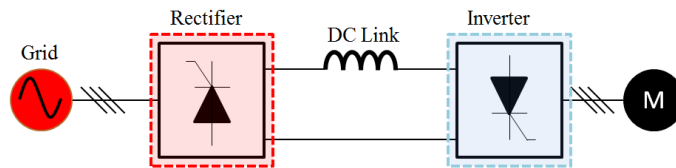


Figure 2.23: CSI structure

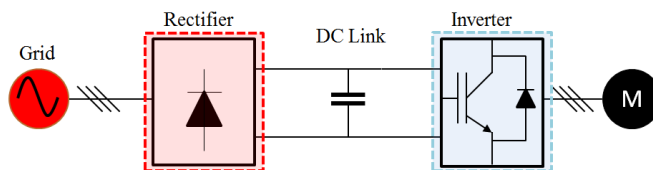


Figure 2.24: VSI structure

Figs. 2.24 and 2.25 illustrate a basic schematic of the LCC and VSC drives. As compared to the VSC drives, the LCC drives are advantageous to use in high power and torque

applications, however current harmonics are introduced that require appropriate mitigation measures, as shown later in the thesis.

By having a 12-pulse configuration the introduced harmonics in the system are minimized. Using (2.6), it can be seen that the order of harmonics present in the system reduce significantly as the ‘pulses’ of converter increase [53].

$$H = kq \pm 1 \quad (2.6)$$

Where H is harmonic number (integer multiple of the fundamental), k is any positive integer, and q is the converter pulse number. A 6-pulse inverter has 5th, 7th, 11th, 13th, etc. harmonics present in the system. However the 12-pulse configuration gets rid of 5th and 7th harmonics, and the system has 11th, 13th, 23rd, 25th, etc. harmonics present.

2.8 LCC STARTING TECHNIQUES

At start-up, the back-emf is not sufficient for natural commutation [6-7] of the thyristors, therefore the motor needs to be run either using a starter motor separately that is decoupled after a speed threshold is achieved, or a starting mechanism must be adopted for ensuring a smooth start. A methodology used by some drive manufacturers allows the drive to start by altering the control angle of the thyristors in the line-side converter to operate in the “inverter” region, or by simply pulsating the angle between, e.g. 60 degree to 150 degrees. This pulsation (also known as pulse-mode operation) allows for the rotor to gain enough speed to begin natural commutations, typically above 6% of nominal

speed. In this thesis, an external VSI is used as a starter until sufficient speed is achieved to allow natural commutation of current through the thyristors. The purpose of this external inverter will be discussed in detail towards the end of the thesis, as it functions as a dual-purpose converter. The VSI, alongside acting as an external starter also acts as an active power filter for harmonics mitigation as will be presented in later sections.

CHAPTER 3. LCC DRIVE CONTROL AND 6-PHASE MOTOR MODELLING

Of all the different types of drives and topologies present, this thesis emphasizes on the LCC drive for an LNG plant Applications [55]. These drives are also known as naturally commutating drives and this natural commutation of current through the thyristors is generally achieved with synchronous machines at speed above 10% of synchronous speed [56-59]. The back-emf is responsible for this commutation; therefore at start-up the back-emf is not sufficient to provide current commutation to the motor bridge. At start-up, the line-side converter may be used as an inverter to have the DC-link current to be zero to enable changing the states of the machine-side thyristors. The start-up is discussed in a later chapter.

The LCC drives have gained great popularity in high power applications (typically up to 100 MW) [59]. The simplicity of the converter design and the maintenance free motor design are common advantages of the LCC drives. Some problems of the LCC drives include introduction of grid current harmonics and torque pulsations at low speeds.

3.1 OPERATION OF LCC

The LCC is a reliable option for an adjustable frequency drive when it comes to high power applications. A simple schematic of the LCC drive system is presented in Fig. 22

earlier. An LCC drive is the source of three-phase currents to the motor. The frequency and the phase of these three-phase currents are synchronized with the position of the rotor. Commutation of the currents in the inverter to supply the right sequence to the motor phases is managed by the back-emf of the motor. The amplitude of the currents however, is dependent on the phase-controlled line side converter with the DC-link inductor L_d . This inductor has two main purposes:

- a. Reducing the current harmonics that are being fed to the machine side converter and the motor eventually, and
- b. Ensuring that the input to the inverter appears as a current source.

By controlling the firing angle of the thyristors in the line-side converter, the DC output voltage can be controlled; therefore controlling the magnitude of the current passing through the inductor L_d . The line-side converter normally operates as a rectifier.

The machine side or load side converter normally operates as an inverter, but is similar to the line side converter in design (thyristor-based). The commutation of current is provided by induced back-emf from the synchronous motor.

In the LCC, the current passing through the DC-link inductor is constant and this means that for power to be transferred from the line side to the machine side, there should be voltage or potential difference between the two sides.

To counter the effect of inter-harmonics, the DC-link inductor and the number of pulses chosen for the converters play a significant role. Harmonic mitigation is more effective

with a higher inductor value and number of pulses. However, this is not the case due to design and cost constraints.

It is important to know that in start-up or at low speeds of operation (below 10% rated speed), the back emf of the synchronous motor might not be sufficient to provide current commutation and therefore, the line-side converter operates as an inverter [18] to force the current passing through the inverter to be zero. This is done in order to provide the turn-off signal to the thyristor gates of the machine-side converter.

3.2 LCC DRIVE TOPOLOGIES

Apart from the topology presented in Fig. 2.11, there are some variations to the LCC drive topologies [61] as shown in Fig. 3.1:

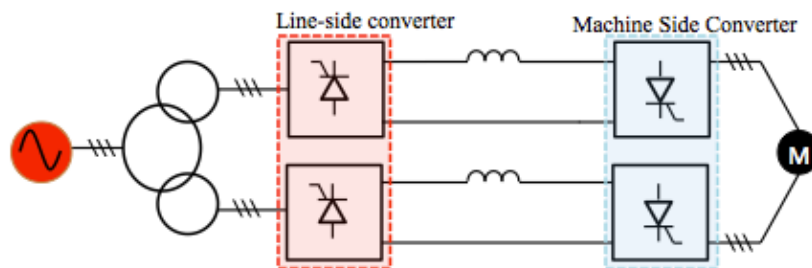


Figure 0.1: LCC drive topology 2

Throughout this thesis, the former LCC drive topology presented in Fig. 2.11 is used in order for the presented cases to resemble the actual drive topology being studied. However, as the thesis progresses, higher order topologies (18,24-pulse) are presented in Appendix A.

3.3 OPERATION AND CONTROL APPROACH

As mentioned in the earlier sections, the terms inverter and rectifier are described in an absolute and generic context. However, the two converters, i.e. line side and machine side, function in a way that the operation can be interchanged at some instances. It has been established thus far that the converters are using thyristors as the switching elements and therefore the control angle (firing angle) is responsible for the operation of the convertor blocks as a rectifier or an inverter.

There can be a number of ways to control [59, 62] the LCC. The type of control adopted in this study is illustrated in the Fig. 3.2 below:

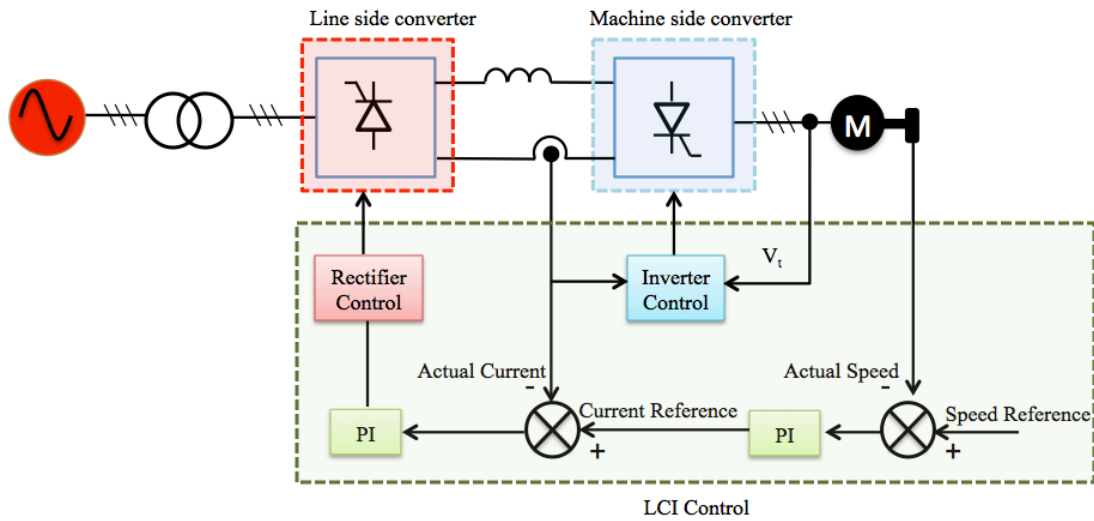


Figure 0.2: General LCC control mechanism

The speed reference is compared to the actual speed of the synchronous motor. Since the speed is related to both flux and the therefore current, a gain is used to obtain the reference current for the system. This is compared with the actual current that is passing through the inductor and the output of the controller is used as feedback to the line side converter. In simple terms, if the actual speed is less than the reference, then the error signal is amplified and the new current reference would be greater than the actual current (I_d). The output from the controller increases the DC link voltage applied, which in turn increases the current, finally providing the increased amount of torque to match the speed reference.

3.4 SIX PHASE MOTOR MODELLING

The multi-phase machine has various advantages over a conventional three-phase machine. For high-power applications such as the one presented in this thesis, a 6-phase motor is commonly used. Further, there are two types of multi-phase [64-65] machines, namely, symmetrical and asymmetrical type. For a symmetrical machine, the stator windings are shifted 60° spatially, whereas the winding shift for asymmetrical machines is 30° as illustrated in Fig. 3.3.

One primary benefit of using multi-phase machines is the fact that for a given rated power, the current per phase is reduced, alongside the reduction of electromagnetic torque ripples. The factor that makes the asymmetrical type more favorable than the symmetrical machine is due to the interferences [64-66] caused in individual phases in symmetrical machines. The asymmetrical model also enabled elimination of the 6th [66] harmonic of the torque ripple, which is caused by the 5th and 7th stator current harmonics.

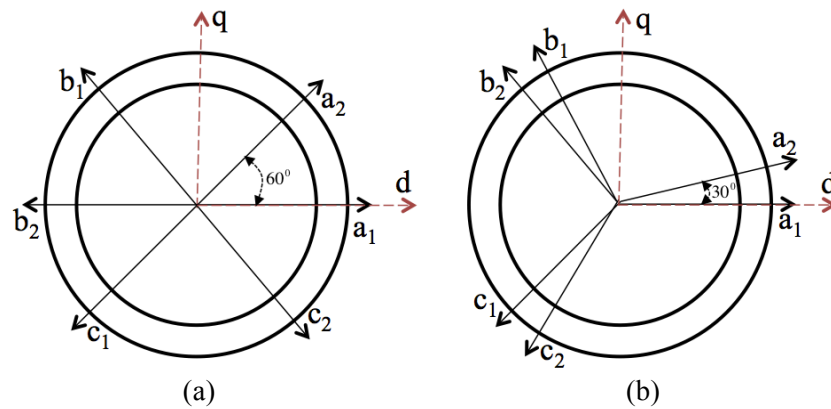


Figure 0.3: 6-phase motor: (a) symmetrical and (b) asymmetrical

Another key advantage of the asymmetric type over the symmetric type is better fault ride through capabilities. In the presence of a fault in one of the phases of the symmetrical machine, a greater de-rating [66] of the machine has to take place as compared to the asymmetric model.

This section will present a mathematical model of the dual three-phase permanent magnet synchronous motor (PMSM), using winding transformation initially. The modeling is performed under the following conditions [40]:

- a. Uniform motor airgap
- b. Uniform magnetic field in air gap
- c. Magnetic saturation of the motor core is neglected and damper windings have been transformed into d-q axis respectively as shown in Fig. 33. Damper windings are used in synchronous motors for two main reasons. One is to assist in self-starting, as these windings are short-circuited and carry current at start-up since

the synchronous motor works as an induction motor during start up. These windings also provide flux compensation in transient fluctuations caused mostly by unbalanced or unsteady loads, resulting in machine reaching synchronism again.

- d. Steady-state current is sinusoidal.

The schematic of a 6-phase motor is presented in Fig. 33, where it is seen that the windings $A_1B_1C_1$ lead windings $A_2B_2C_2$ by 30° (spatial electrical degrees). The two windings produce identical fundamental magnetomotive force (MMF) in the air gap; therefore resultant for a 6-phase motor is the summation of the both. Transforming from six-phase to equivalent three-phase model, number of turns are added, therefore the phase voltage doubles, however phase current remains the same.

$$i_A = i_{A1} \quad (3.1)$$

$$u_A = 2u_{A1} \quad (3.2)$$

Where i_{A1} and u_{A1} represent the phase current and voltage of the dual three-phase machine, and i_A and u_A represent the phase current and voltage of equivalent three-phase machine respectively.

Supposing that the stator resistance and leakage inductance per phase for the 6-phase motor is R_{s1} and L_{s1} , and d-q axis armature reaction inductances are L_{ad1} and L_{aq1} respectively. Then, the equivalent resistance and inductances for the equivalent three-phase motor are given by:

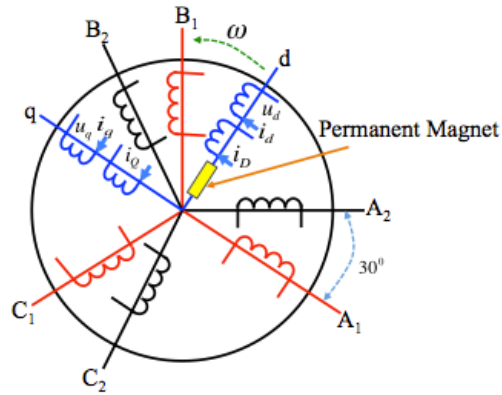


Figure 0.4: Six phase motor illustration

$$R_s = 2 R_{s1}$$

$$L_s = 2 L_{s1}$$

(3.3)

$$L_{ad} = 2 L_{ad1}$$

$$L_{aq} = 2 L_{aq1}$$

Equations presented (7-9) are equivalent mathematical representations of a three-phase PMSM derived from a six-phase PMSM.

3.5.1 SIX-PHASE SYNCHRONOUS MOTOR MODEL IN SYNCHRONOUSLY ROTATING REFERENCE FRAME

Presenting the three-phase windings in equivalent d-q representation [67], and as shown in Fig. 3.4, the d-q coordinates and the rotor (depicted by the use of a magnet) rotate with the same angular speed. The equivalent three-phase motor model in d-q frame is

presented as follows. Voltage equations are presented in (3.4), flux linkage in (3.5) and torque equations in (3.6).

$$\begin{aligned}
 u_d &= R_s i_d + p\psi_d - \omega\psi_q \\
 u_q &= R_s i_q + p\psi_q - \omega\psi_d \\
 0 &= R_D i_D + p\psi_D \\
 0 &= R_Q i_Q + p\psi_Q
 \end{aligned} \tag{3.4}$$

$$\begin{aligned}
 \psi_d &= L_{sd} i_d + L_{md} i_D + \psi_f \\
 \psi_q &= L_{sq} i_q + L_{mq} i_Q
 \end{aligned} \tag{3.5}$$

$$\psi_D = L_{mD} i_d + L_{rD} i_D + \psi_f$$

$$\psi_Q = L_{mQ} i_q + L_{rQ} i_Q$$

$$T_e = n_p (\psi_d i_q - \psi_q i_d)$$

$$T_e = n_p (\psi_f i_q + (L_{sd} - L_{sq}) i_d i_q + (L_{md} i_D i_q - L_{mq} i_d i_Q)) \tag{3.6}$$

$$T_e = \frac{J}{n_p} \frac{d\omega}{dt} + T_L$$

$$\omega = p\phi$$

Where the abbreviations are as follows:

L_{md} , L_{mq} : Stator and damper winding mutual inductance in d-axis and q-axis respectively

L_{sd} : Self-inductance of equivalent two-phase stator windings in d-axis

L_{sq} : Self-inductance of equivalent two-phase stator windings in q-axis

L_{rD}, L_{rQ} : Damper windings self-inductance in d axis and q-axis respectively

ψ_f : Permanent magnet flux linkage

ω : Rotating speed of the rotor and d and q coordinates

ϕ : Electrical degrees by which d axis leads phase A1

n_p : Number of Poles

3.5.2 SIMULATION CONSIDERATIONS

As presented in earlier sections, the actual motor design is of asymmetrical type, with the stator winding spatially shifted by 30° . Furthermore, in regards to the control schematic that is simulated in this thesis, the motor current is used as an input, as illustrated in Fig. 3.2. For control purposes, the d-q coordinates of the motor current are used as available in the machine model from Simulink. However, in reality there are two different sets of d-q responses from the stator of the 6-phase machine.

It is critical to understand that the motor model can be distributed into three orthogonal frames [68], namely α - β , x-y, and zero-sequence frames. Where, α - β frame is the fundamental frame that provides electromechanical energy conversion. The x-y frame, also known as the losses or harmonics frame, therefore does not contribute to the computations, since the motor current component i_q is used in the control schematic as illustrated in Fig. 3.2.

Finally, a 6-phase machine is not used, and a dual-secondary coupling transformer is used on the output of the machine-side converter in order to couple the 6-phase output from the 2x6 pulse machine side converter to a 3-phase PMSM.

CHAPTER 4 . SIMULATION RESULTS

This section will present all the different phases during the design and simulation of the LCC drive system. All the building blocks of the complete LCC drive are presented in this section alongside the respective results.

4.1 RECTIFIER STAGE

This is the first block that interfaces the drive to the utility or the power grid alongside the transformer. A 6-pulse rectifier is implemented in Simulink, which is further developed into a 12-pulse converter to match the system under study. This is also useful to present the output of the converter with a varying control angle. Note that for this example a fixed control angle is demonstrated and the different outputs are presented.

The pulse generator is an in-built Simulink block that was used where the control angle is chosen to be a constant, and the frequency is obtained from a phase-locked loop block to match the frequency of the voltage instantaneously.

An input to the pulse generator block is the control angle for the thyristor gates, which was obtained using the control as shown in Fig. 4.1.

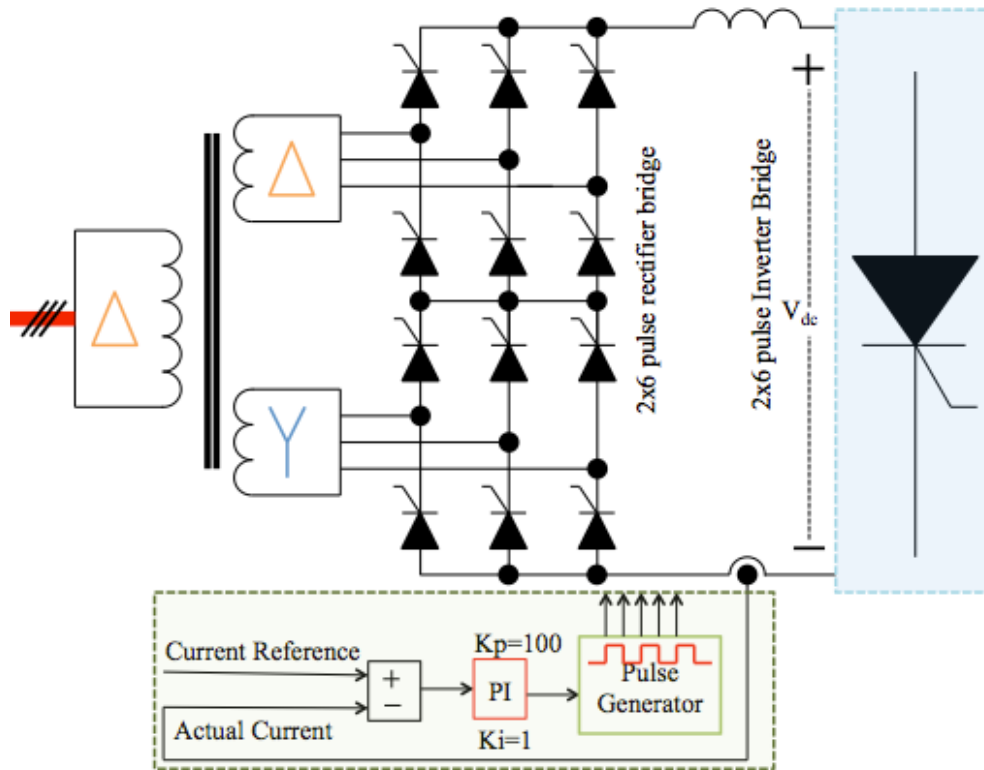


Figure 4.1: 12 Pulse Rectifier configuration with current control

Plots of the output voltage of the rectifier block with varying control angles are presented below, as well as the current-controlled case. The results are shown for both 6-pulse and 12-pulse rectifier simulations.

As shown in Fig. 4.1, a Proportional Integral (PI) controller is used to control the current. The error signal from the difference of actual and a reference current is passed through the PI controller to achieve a zero error condition and consequently track the reference signal adequately. It is to be noted that the control parameters are chosen by trial and error.

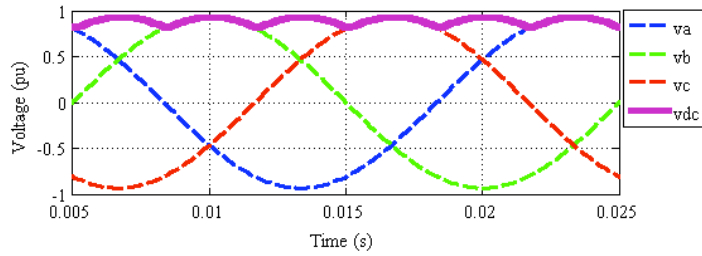


Figure 4.2: Rectified voltage at 0 degrees for 6-pulse rectifier

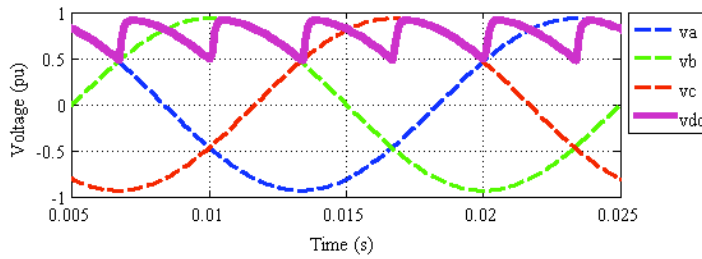


Figure 4.3: Rectified voltage at 30 degrees for 6-pulse rectifier

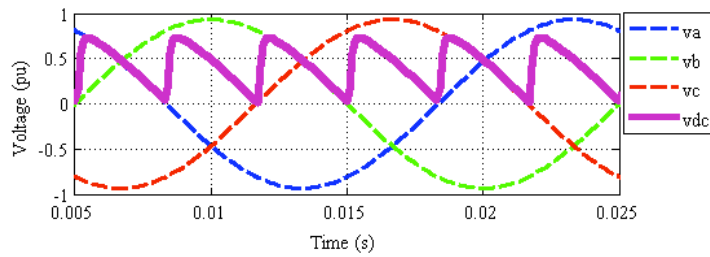


Figure 4.4: Rectified voltage at 60 degrees for 6-pulse rectifier

The results of the rectified voltage as shown in Figs. 4.2-4.4 are in accordance with theory. The DC output from the rectifier block is fed to the inverter block through a

reactor or an inductor (DC-link). If the same is done for the 12-pulse rectifier block as shown in Fig. 4.1, the following is obtained:

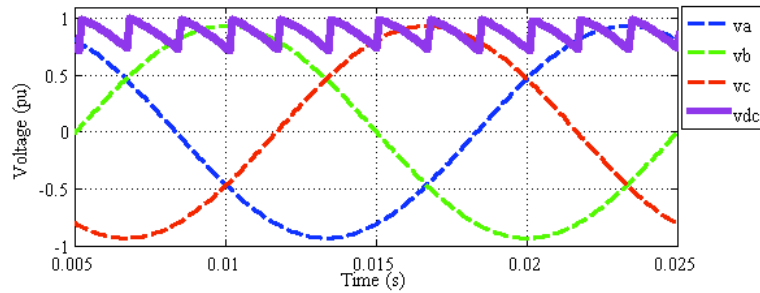


Figure 4.5: Rectified voltage at 0 degrees for 12-pulse rectifier

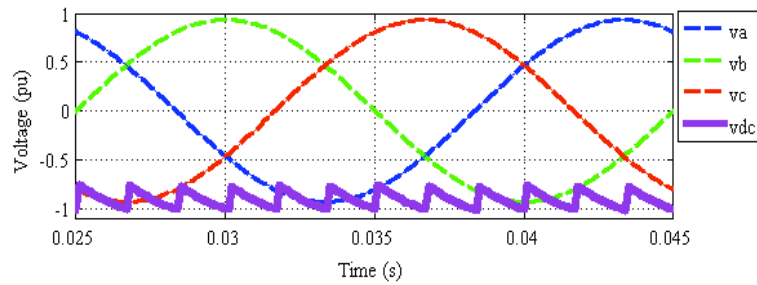


Figure 4.6: Rectified voltage at 180 degrees for 12-pulse rectifier

4.1.2 RECTIFIER WITH CURRENT CONTROL

Apart from having a free running rectifier block, a simple control system is established to regulate the current output from the thyristor block. In a complete back-to-back system,

this current would be the DC-link current. The system parameters are similar to the ones mentioned in table 4.1.

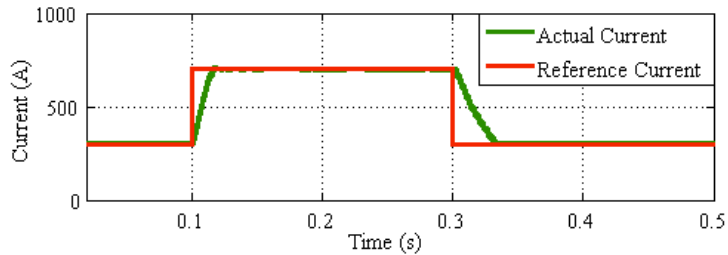


Figure 4.7: Current control implemented in rectifier Block

As seen from Fig. 4.7, the current controller allows the rectifier module to track the reference well. The same controller concepts are implemented at 12-pulse and back-to-back configurations. Control parameters of the PI controller can be set using different methods, however in this case a trial and error approach was used to obtain a system where the actual current tracks the reference well. The parameters were set primarily to achieve minimum over-shoot and quick response to the changes to the reference.

4.2 INVERTER

To model the inverter block, the following schematic is simulated. The simulation block can be seen in the appendix C, however it is to be noted that the simulations performed in this thesis use 3-phase PMSM as the load.

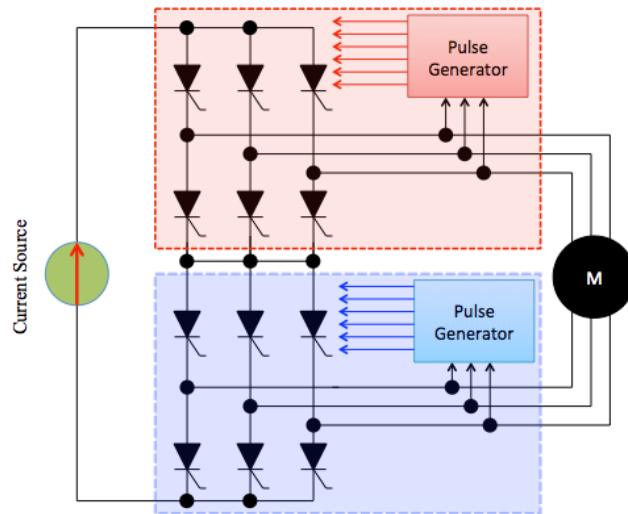


Figure 4.8: 12-pulse inverter schematic

The schematic shown in Fig. 4.8 presents only a free running system with no proper feedback controlling the firing angle of thyristors. A control system would be introduced later on in this section to demonstrate the control philosophy and its simulation and results.

For the simple 6-pulse configuration, an external voltage source is used for a short time period in order to start the machine, and then disconnected to let the LCI run by natural commutation of thyristors. Fig. 4.9 illustrates the voltage build-up before and after the external voltage source is cut-off using a three-phase breaker. In order to ensure that the thyristors are functioning well, different control angles are used for the firing of the thyristors and the voltage varied within a range, alongside the motor speed, which is a primary output parameter.

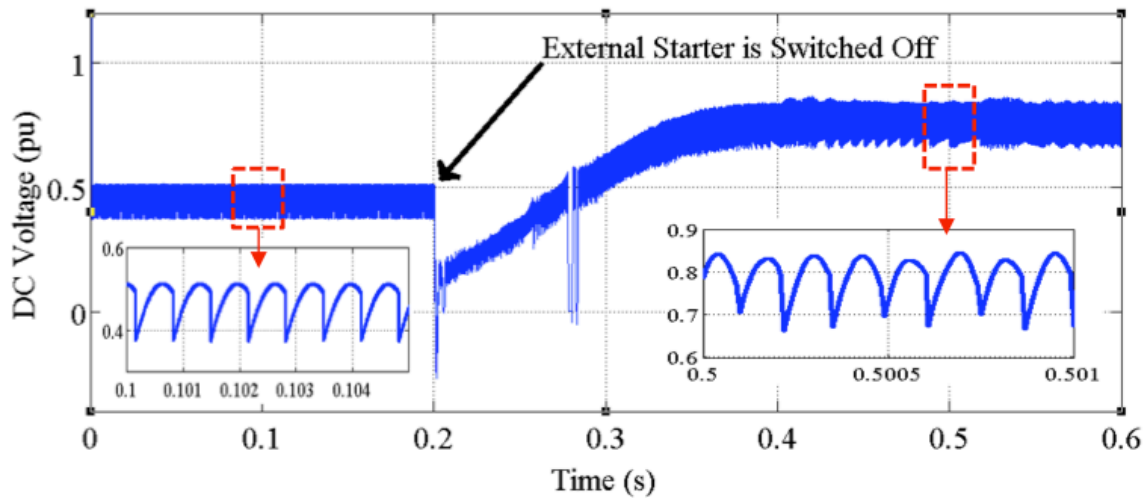


Figure 4.9: LCI input voltage waveform

For the simulation of the inverter block, a PMSM is used as the primary load. A constant mechanical torque is applied as an input to the synchronous machine and the rotor speed is presented in Fig. 4.10. As the external starter goes off, the motor starts operating at a higher speed as compared to when the starter is present. The starter provides adequate motion to have back emf sufficient to allow natural commutation of the thyristors. This example presents a freely running system with no speed control, however this speed is regulated as shown in later sections. The increased speed can also be verified by the increased frequency of the voltage waveform shown in Fig. 4.9. The results presented in this section are corresponding to the following motor/system parameters:

Table 4.1: Motor Parameters

Motor Parameters	Value
Rated Power	8 MW
Rated Voltage	3 kV
Number of Phases	3
Transformer Primary Voltage	33 kV
Transformer Secondary Voltage	3.3 kV
Back EMF Waveform	Sinusoidal
Stator Resistance (Ohms)	0.2
Flux Linkage (V.s)	0.175
Inertia (kg.m ²)	0.9
Viscous Damping (N.m.s)	0.005
Poles	2
Rated Speed	3000 rpm

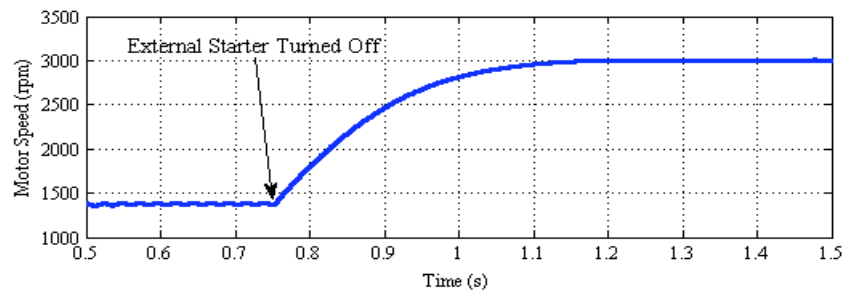


Figure 4.10: Motor speed

Fig. 4.10 presents the speed response using the external starter and shows the instance when the starter is cut-off and the LCI drives the load independently. The starting speed is presented at steady state only. After testing the open loop operation as shown above, the speed control is established further.

4.3 SPEED CONTROL

As shown in the Fig. 4.11, the errors signal from the speed difference is passed through a PI controller and the actual current component (I_q) is compared to the current reference. The output is again passed through the PI controller in order to achieve the right control angle to achieve the desired current, which in turn provides the desired speed.

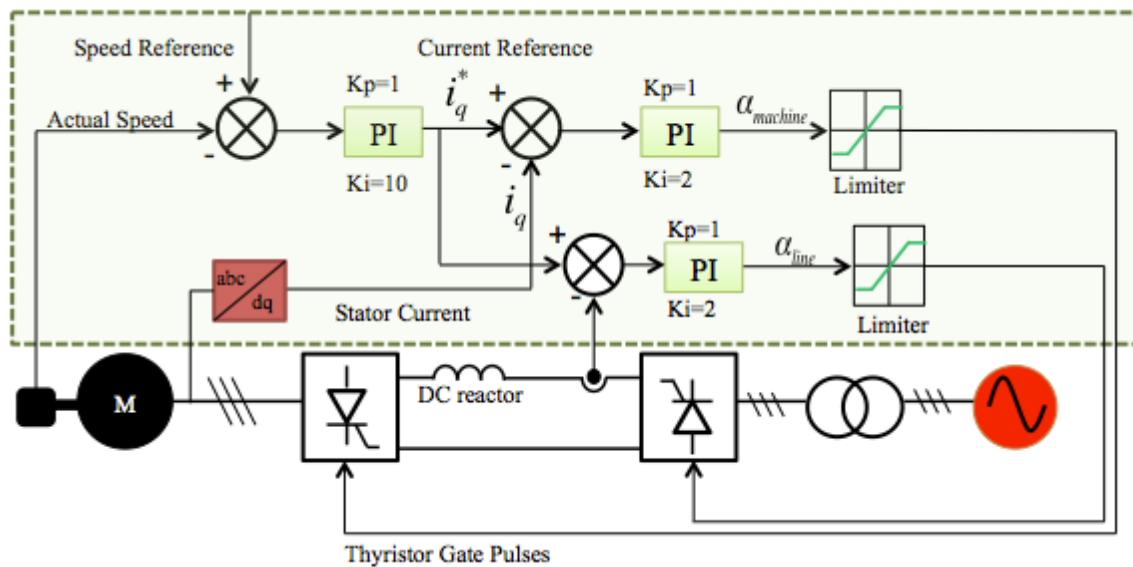


Figure 4.11: Control angle feedback block diagram

This methodology is implemented in Simulink, and speed references of different steps are applied to the system. As presented in the Fig. 4.12, the speed reference is well tracked with the help of this speed controller. More details regarding the LCC control are presented in Appendix C.

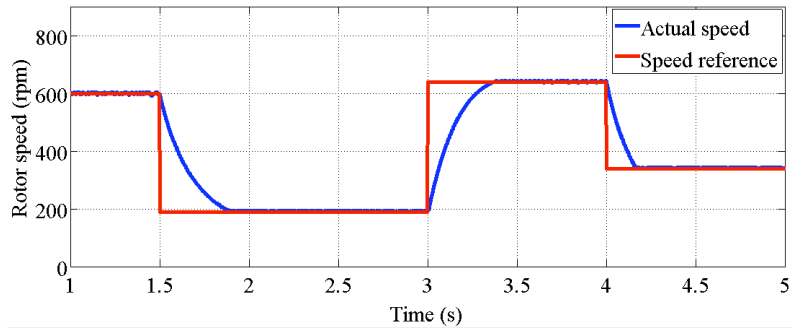


Figure 4.12: Speed response with controller

The control parameters for the proportional and integral gains are provided in Table 4.2. The controller has high bandwidth as the current control parameters have a faster response than those of speed control, in order for the inner loop to be faster than the outer loop and enable rejection of disturbances before they propagate to the outer loop.

Table 4.2: Controller gains

Control	K_i	K_p
Speed	10	1
Current	2	1

Since the control methodology successfully tracked the speed references provided at 6-pulse topology, it was further developed into a complete back-to-back system with both line and machine side converters being used in a 12-pulse topology.

The schematic for the 12-pulse LCC configuration is illustrated in Fig. 4.13.

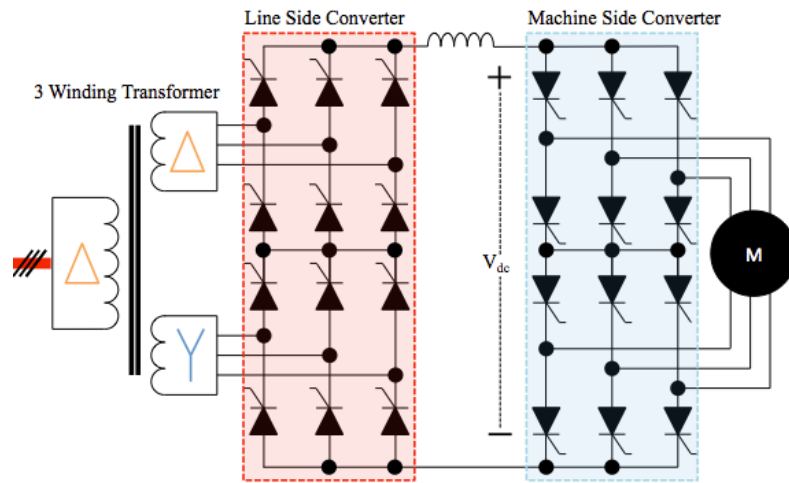


Figure 4.13: Schematic for back-to-back converter configuration

There are various configurations for the LCI drive; however this simple model is used for the simulation in this section. The control mechanism as illustrated in Fig. 4.8 is used at the 12-pulse topology as well. In this model, the voltage is stepped down to a level of around 3kV (as shown in table 4.1) on both the secondary windings, where it is input to the line-side thyristors.

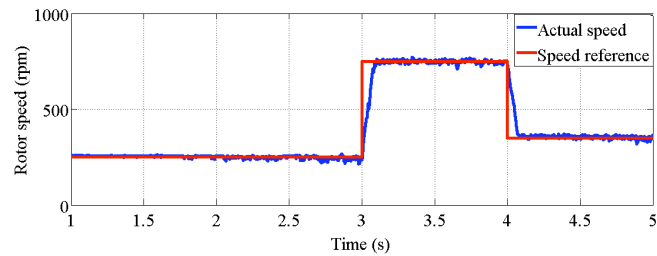


Figure 4.14: Speed response with modified controller gains

Fig. 4.14 presents the speed controller test results, where the actual motor speed tracks the desired reference as specified. A brief description of the rectifier (line side converter) thyristor pulses is presented in the appendix B.

4.3.1 LCC OPERATION WITH CONSTANT SPEED VARIABLE TORQUE

This section illustrates the system response where the torque requirement is altered during operation, as the previous cases of speed control were presented under constant torque. This is critical to perform, as it will demonstrate the robustness of the speed controller and present a real life scenario.

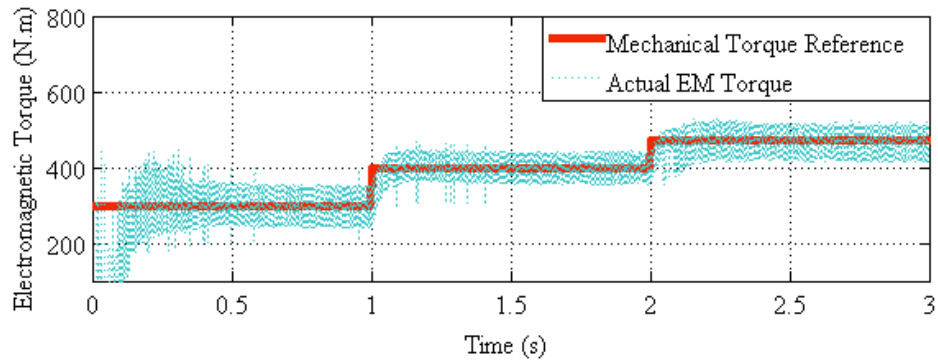


Figure 4.15: Improved electromagnetic torque response of motor

The mechanical torque or the torque demand is variable as shown in Fig. 4.12; however the speed is maintained constant. This case is analogous to actual scenarios where the load feedback from the turbine is variable, however the motor is to be run at a desired constant speed.

Similar to Fig. 4.14, the speed response presented in Fig. 4.16 tracks the reference well and the torque fluctuations as shown in Fig. 4.15 do not affect the speed response of the motor. The response was similar even with higher torque references.

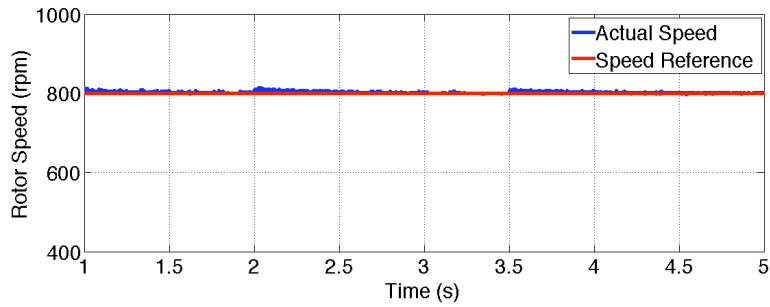


Figure 4.16: Speed response with incremental mechanical torque

This section presents the case closely related to actual scenarios where the LCC drive is used in a speed and torque controlled manner. Fig. 4.17 shows the stator currents where the steps of a 12-pulse converter can be visually seen. The shown current waveform is for the constant speed operation of the LCC drive.

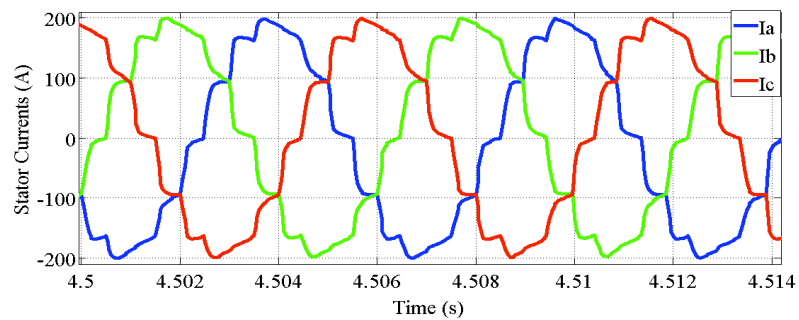


Figure 4.17: Stator currents at constant speed operation

The results of this section show that the speed response of the machine is well controlled using the LCI drive, as shown in Figs. 4.11-4.13. The speeds are presented for varying ranges of torque and the speed tracking is satisfactorily accomplished.

CHAPTER 5 . MITIGATION OF HARMONICS

5.1 HARMONICS

As discussed prior to this section, harmonics are great problems associated to the LCC drives, and non-linear loads as presented in this thesis. The presence of non-linear loads can be generalized to the equipment/components that have non-linear voltage and current characteristics, such as, VFDs, transformers, electrical motors, etc. The power providers are committed to providing voltages with low distortion, and the client is responsible to lower the current harmonics being injected back to the grid. For the healthiness of this mutual power loop, it is critical from the customer's perspective to manage the current harmonics being re-injected to the grid [70].

The standard term used to refer to the harmonic content present in the voltage/current waveforms is known as total harmonic distortion (THD). THD is basically the ratio of the rms value of the harmonic components to the rms value of the fundamental component of the measured parameter. The points at which THD measurements are of importance in this thesis are at the primary winding of the utility transformer feeding the LCI drive/motor. Following section will be illustrating the THD plots of the grid currents with different topologies and additional filters.

5.2 POWER FACTOR

In sinusoidal voltage/current waveforms, the active power component is defined as the product of the voltage and current components, and reflects the actual or useful power being transferred. Reactive power is the component that is orthogonal to the active power component and it does not cause real flow of energy, albeit increasing the steady-state current [70-72]. In mentioned scenario, the power factor is resultant vector of the active and reactive power vectors, however due to the presence of non-linearities; the definition of power factor varies as shown below.

Loading power and power factor

Loading power [70, 73] can be broken down into active and fictitious power components. Where active power contributes to real flow of energy, reactive power does not do so, rather it increases steady-state currents in sinusoidal systems. Fictitious power includes all the components causing the loading power to exceed active power. Furthermore, the fictitious power can be split into reactive and deactive components, also known as uncorrelated fictitious power. Reactive power also has two components, namely the fundamental, which is the cross product of fundamental current and voltage components, and the residual, which accounts for the difference between reactive and fundamental reactive power. The presence of non-linearity of loads does not allow the representation of non-fundamental currents to be represented in a two-dimensional coordinate system. Therefore, the currents components are divided into orthogonal components namely, the active, reactive, and distorted components [73].

Displacement factor:

Having reactive components in the load leads to reactive currents to flow alongside the resistive current components. The current can lead or lag the voltage waveforms depending on the load being either capacitive or inductive, respectively. The displacement factor is due to the phase shift between the voltage and resultant current at the fundamental frequency.

$$DisplacementFactor = \cos(\theta) \quad (5.1)$$

Where θ is the angle between the voltage and current at the fundamental frequency.

For the rectifiers, the displacement factor equals the cosine of the firing angle (α), and the following holds:

$$S = \sqrt{P^2 + Q^2} \quad (5.2)$$

$$P \propto \cos(\alpha) \quad (5.3)$$

$$Q \propto \sin(\alpha) \quad (5.4)$$

From (5.3-5.4), it can be seen that as the firing angle (α) equals 90 degrees, the active power approaches zero, and reactive power is at its maximum. For this reason, it is not desirable to have the firing angle close to 90°.

Distortion factor:

Since there is a presence of non-linear loads, in order to measure power factor, the presence of harmonics in the system needs to be taken into consideration [71].

$$DistortionFactor = \frac{1}{\sqrt{(1+THD^2)}} \quad (5.5)$$

The equation to calculate the power factor in the system can be written as follows:

$$Power\ factor = (Displacement\ factor).(Distortion\ factor) \quad (5.6)$$

5.3 6-pulse topology

To emphasize the effect of 12-pulse topology (as presented in this thesis), the harmonics and the THD of the utility side current is presented in Fig. 5.1 and 5.2, where the frequency spectrum of the line side current is illustrated with a 6-pulse converter topology and the subsequent use of a single-phase transformer, as shown earlier in Fig. 2.17.

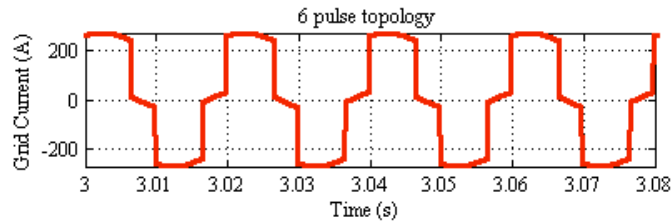


Figure 5.1: Grid current with 6-pulse topology

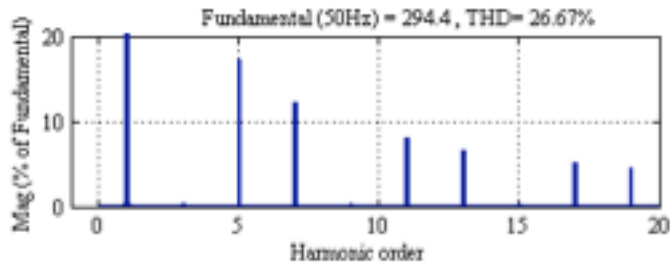


Figure 5.2: THD with 6-pulse system

The harmonic content is quite high as 5th, 7th, 11th, 13th, 17th and 19th order harmonics are present in the system [2], contributing to a THD of 27%. It is to be noted that no triplen harmonics (3rd, 6th, 9th...) are present, due to the balanced three-phase system.

5.4 12-PULSE TOPOLOGY

Despite having a multi-phase transformer and 12-pulse converter topology, there is still a presence of 11th and 13th order harmonics at the utility/line side as illustrated in fig. 5.3/5.4. This accounts for the THD of approximately 15% and can be improved as shown in the following section.

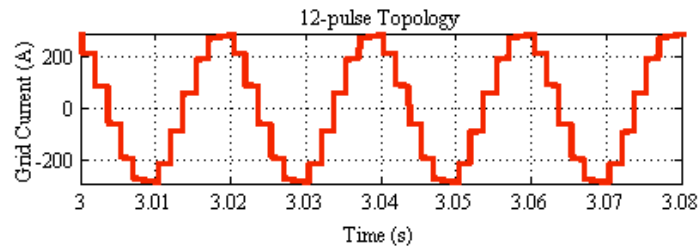


Figure 5.3: Grid current with 12-pulse topology

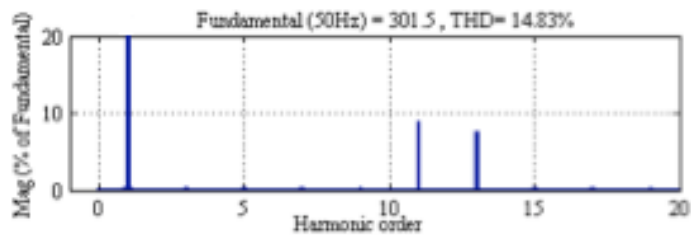


Figure 5.4: Grid current THD with 12-pulse topology

5.5 12-PULSE TOPOLOGY WITH PASSIVE FILTER

The current waveforms in Fig. 5.3/5.4 is the system employed currently in the specific case being studied in this thesis, and it is seen that even though it's better than the 6-pulse configuration, there is room for improvement in the power quality at the utility side. Using an appropriate passive filter, the 11th and 13th harmonics content (as shown in Fig. 5.5) can be removed, resulting in better THD measurements as shown below:

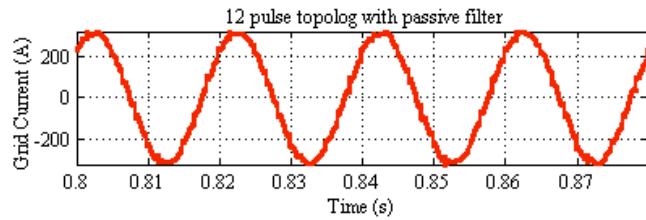


Figure 5.5: Grid current with 12-pulse topology with input filter

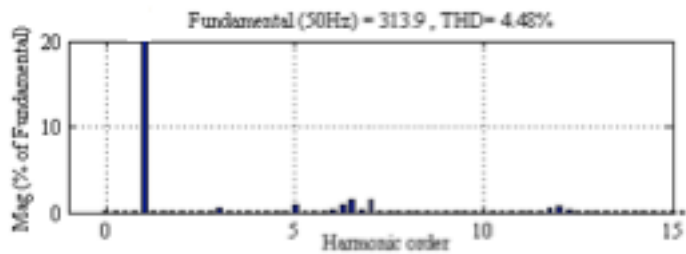


Figure 5.6: THD with 12-pulse topology with passive filter

The passive filters for this application can have multiple designs. Filter banks as illustrated in Fig. 5.7, consisting of series LC components for 11th and 13th harmonics are used in this thesis. The plots illustrated in Figs. 5.5/5.6 use simple LC filter banks to attenuate 11th and 13th harmonics in specific, and the attenuation is quite visible as compared to former plots without a filter.

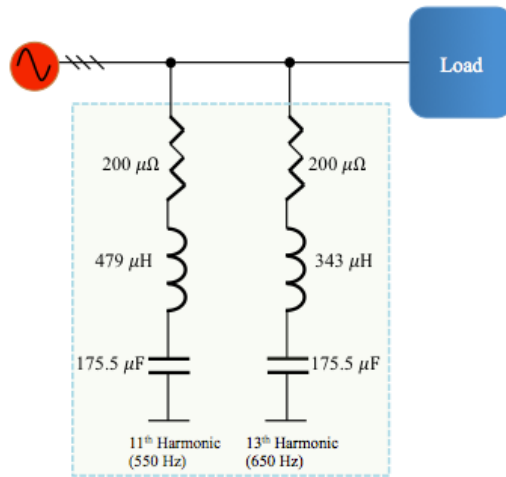


Figure 5.7: Passive filter configuration

The cut-off frequency is obtained by the following expression:

$$f_{cut-off} = \frac{1}{2\pi\sqrt{LC}}$$

Filter parameters for 11th Harmonics (550 Hz):

$$\begin{aligned} \mathbf{R} &= \mathbf{20\ \Omega} \\ \mathbf{C} &= \mathbf{175.5\ \mu F} \\ \mathbf{L} &= \mathbf{479\ \mu H} \end{aligned}$$

Filter parameters for 13th Harmonics (650 Hz):

$$\begin{aligned} \mathbf{R} &= \mathbf{20\ \Omega} \\ \mathbf{C} &= \mathbf{175.5\ \mu F} \\ \mathbf{L} &= \mathbf{343\ \mu H} \end{aligned}$$

As presented in Fig. 5.6, the THD was brought down to 4.48%, compared to the 15% where no input filter was used, and 11th and 13th harmonics were greatly reduced.

5.6 24-PULSE TOPOLOGY

Another presented case is for a 24-pulse system with both line and machine side converters having 24 thyristors each. The schematic can be viewed in appendix A, and the results are shown in Fig. 5.8/5.9.

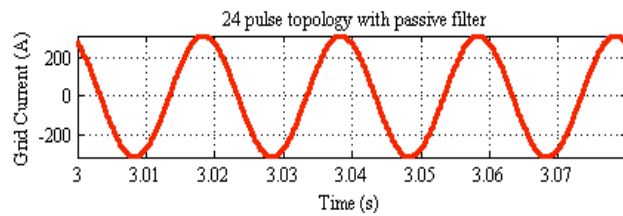


Figure 5.8: Grid current with 24-pulse topology

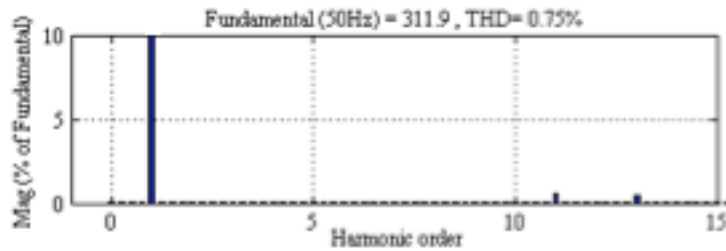


Figure 5.9: THD with 24-pulse topology

The 24-pulse topology is used with a passive filter at the input side. For clarity, the schematics of the presented topologies are shown in Appendix A.

A summary of the THDs and power factors, alongside different topologies that are presented in this section is shown in Table 5.1.

Table 5.1: THD comparison with different topologies

#	Topology	THD on Line Current	% Improvement	Power Factor
1	6-pulse converter	29.1 %	-	
2	12-pulse converter (a)	14.8 %	49%	0.96
3	12-pulse converter (b)	13.2 %	54%	0.96
4	12-pulse converter with passive filter	4.48%	83%	0.97
6	24-pulse with passive filter	0.75%	97%	0.98

CHAPTER 6 . ACTIVE POWER FILTER

6.1 Introduction

The previous section demonstrated different topologies and varying THDs at the utility side. The input filters used were passive filters and the lowest THD was obtained with a 24-pulse topology and a passive RLC filter at the input side. This section presents an Active Power Filter (APF) to have a better control over the harmonics on the utility/grid side, as well as the reactive power. APFs are used in power systems to reduce harmonics, compensate reactive power and neutral currents if parallel connected. These filters might be employed to mitigate voltage harmonics and balance voltages in an un-balanced system if series-connected [74].

As compared to passive filters, APFs have improved harmonic compensation characteristics [74-76], as the impedance varies according to the AC grid, and frequency varies as per the harmonic current components. To achieve this harmonics and VAR compensation a PWM based inverter is generally used, where a VSI has regulated DC voltage on the DC-capacitor, and the CSI has regulated DC current across the inductor.

6.1.1 ACTIVE FILTER OVER PASSIVE FILTER

This section presents factors that lead to the introduction of an APF to the drive system. As presented in the previous section, the passive filters provided adequate harmonic filtering, where 11th and 13th harmonics were primarily minimized.

Some of the drawbacks of passive filters are described as follows:

1. An increase in harmonic currents might lead the filter to be overloaded.
2. Overvoltage problems occur due to the parallel resonance [70] between source and the filter.
3. As the RLC filter elements age, detuning of the filter occurs and might require component replacement.
4. The operational frequency of the AC system varies depending on the load and this is to be taken into account while designing the passive filter
5. Passive filters are designed to only mitigate frequencies they are tuned to, and therefore unnecessary frequency component might go undetected.
6. The passive filter should be rated considering that both fundamental and harmonic components will be flowing through the filter.

Some general drawbacks of the APF are as follows:

1. Higher starting and operational costs
2. Higher losses and complexity as compared to passive filters
3. Design restriction in terms of high power ratings and dynamic current response.

For demonstration purposes, the 12-pulse topology is being presented. A general schematic showing the implementation of active power filters for harmonic mitigation and power quality improvement is presented below:

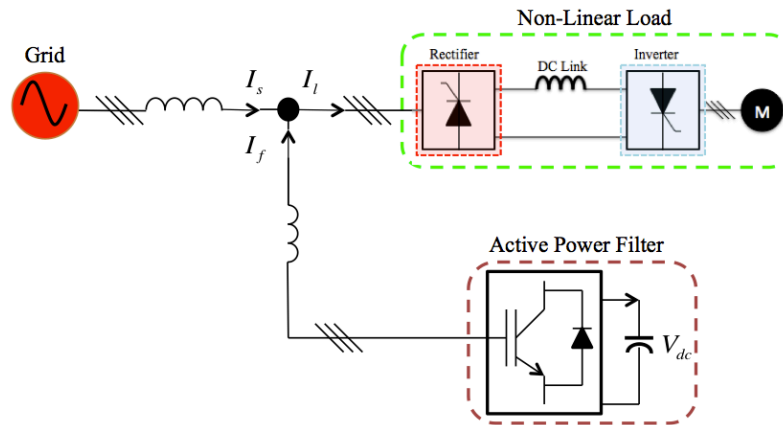


Figure 6.1: Active power filter schematic

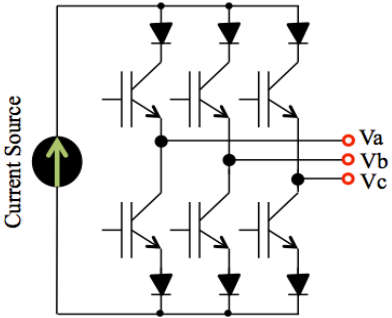
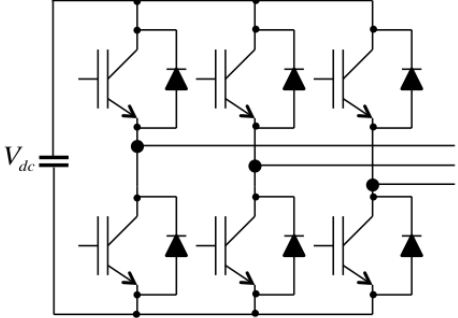
As shown in Fig. 6.1, the APF can be connected parallel to the non-linear load (LCC drive and SM) and the inverter could be either a CSI or VSI type. This thesis presents a VSI type for the APF due to its suitability in the specific application as summarized in Table 6.1. Using an APF over a passive filter allows the system to cancel harmonics, and to supply active power components while cancelling the reactive power component.

APFs can be classified in categories such as series, shunt or a combination of both [73].

6.1.2 CSI APF vs VSI APF

A brief and general comparison between current source APF and voltage source APF is presented in Table 6.1.

Table 6.1: Current and voltage source inverter APF

	Current Source Inverter APF (CSI APF)	Voltage Source Inverter APF (VSI APF)
Topology		
Advantages	<p>It acts as a non-sinusoidal current source providing harmonic current compensation for non-linear loads. This type of APF is quite reliable however; the losses and the inductance are high as well.</p>	<p>The VSI type is quite prominently being used as an APF due to lower cost and the option to expand to multi-level operation [46], such as cascaded bridge, diode clamp or flying capacitor structures.</p>

6.1.3 SHUNT APF VS SERIES APF

A comparison between shunt and series active power filters is presented in Table 6.2.

Table 6.2: Shunt and series APF comparison

	Shunt APF	Series APF
Topology		
Compensation	<p>The shunt APF carries the compensation current components alongside the fundamental current component [73] for compensation of losses, while maintaining a steady voltage across the DC capacitor. Shunt APF acts as a current source.</p>	<p>Unlike the shunt APF, the series APF doesn't compensate load current harmonics, however it provides high impedance to the harmonic current components from the source. Series APF acts as a voltage source.</p>
General Comments	<p>This type of APF can be used for both harmonic reduction and reactive power compensation. The shunt APF might not be able to mitigate the harmonics, and may cause issues related to introducing a DC ripple, and therefore a series inductance is required alongside a shunt APF</p>	<p>As compared to the shunt APF, the series APF are not very common for industrial use, as they have to handle the high current ratings of the load. An advantage of this type of filter is the ability to mitigate voltage harmonics and balance the voltages at the point of common coupling (PCC).</p>
Function	<p>Primary function is to filter current harmonics, reactive current compensation and current imbalance mitigation.</p>	<p>Primarily function is to reduce voltage harmonics, voltage imbalance mitigation, reactive current compensation, and current imbalance mitigation.</p>
Load Type	<p>Used with inductive/current source loads</p>	<p>Used with capacitive/voltage source loads</p>

6.2 HARMONIC CURRENT EXTRACTION

Various techniques exist for the extraction of harmonic currents, and some are presented in this section followed by the technique used in this thesis. The current extraction techniques can be based on time or frequency domains.

1. P-Q Theory

Also known as the instantaneous power or reactive power theory [77] uses Clarke transformation and therefore voltage and currents can be written as shown in (6.1).

$$\begin{pmatrix} v_\alpha \\ v_\beta \\ v_0 \end{pmatrix} = \sqrt{\frac{2}{3}} \begin{pmatrix} 1 & \frac{-1}{2} & \frac{-1}{2} \\ 0 & \frac{\sqrt{3}}{2} & \frac{-\sqrt{3}}{2} \\ \frac{1}{\sqrt{2}} & \frac{1}{\sqrt{2}} & \frac{1}{\sqrt{2}} \end{pmatrix} \begin{pmatrix} v_a \\ v_b \\ v_c \end{pmatrix}, \quad \begin{pmatrix} i_\alpha \\ i_\beta \\ i_0 \end{pmatrix} = \sqrt{\frac{2}{3}} \begin{pmatrix} 1 & \frac{-1}{2} & \frac{-1}{2} \\ 0 & \frac{\sqrt{3}}{2} & \frac{-\sqrt{3}}{2} \\ \frac{1}{\sqrt{2}} & \frac{1}{\sqrt{2}} & \frac{1}{\sqrt{2}} \end{pmatrix} \begin{pmatrix} i_a \\ i_b \\ i_c \end{pmatrix} \quad (6.1)$$

For a three-phase, three wire system, the instantaneous active power and reactive power in $\alpha - \beta$ coordinates can be written as (6.2) and (6.3) respectively:

$$p = v_\alpha i_\alpha + v_\beta i_\beta = \tilde{p} + \bar{p} \quad (6.2)$$

$$q = v_\alpha i_\beta - v_\beta i_\alpha = \tilde{q} + \bar{q} \quad (6.3)$$

Where \tilde{p} and \tilde{q} are alternating active and reactive power components respectively. \bar{p} and \bar{q} are average instantaneous active and reactive power components respectively.

Alternating active and reactive power components are undesirable and can be extracted by filtering the reactive power [77]. For non-linear three-phase loads, compensating currents can be written as:

$$\begin{pmatrix} i_{c\alpha} \\ i_{c\beta} \end{pmatrix} = \begin{pmatrix} v_\alpha & v_\beta \\ -v_\beta & v_\alpha \end{pmatrix}^{-1} \begin{pmatrix} \tilde{p} \\ q \text{ or } \tilde{q} \end{pmatrix} \quad (6.4)$$

2. Synchronous reference frame

In this technique the load currents are transformed into the synchronous rotating frame (d-q) as shown in (6.5):

$$\begin{pmatrix} i_d \\ i_q \end{pmatrix} = \frac{2}{3} \begin{pmatrix} \sin\theta & \sin(\theta - \frac{2\pi}{3}) & \sin(\theta + \frac{2\pi}{3}) \\ \cos\theta & \cos(\theta - \frac{2\pi}{3}) & \sin(\theta + \frac{2\pi}{3}) \end{pmatrix}^{-1} \begin{pmatrix} i_a \\ i_b \\ i_c \end{pmatrix} \quad (6.5)$$

Where θ is the rotation angle of d-q coordinates which is equivalent to ωt . The d-q components of current characterize active and reactive power components of current respectively. Current components are then split to fundamental and harmonic/reactive components.

3. Capacitor voltage control

This method uses regulation of capacitor voltage for extraction of harmonics [71-72]. This technique uses power balance, where the real load power and inverter losses should equal the source real power. For this power balance to be maintained, the capacitor must instantaneously provide compensation.

with the voltage references and using inverse park transformation, alongside a PWM generator, the gate signals are generated. The THD for the supply current with a standard 12-pulse topology is 14 %. With an LCL passive filter this topology provided a THD of about 6 %. To implement the APF, the phase voltage that is input at the drive end was 6kV. The parameters are summarized below:

Table 6.3: APF testing parameters

Source Phase voltage	6 kV
DC-voltage reference	15 kV
Line Inductance	1 mH
Capacitor	3 mF
Switching frequency	4 kHz

The DC reference of 15 kV was fully tracked by the control and the plots of actual voltage and current of the VSI are presented below.

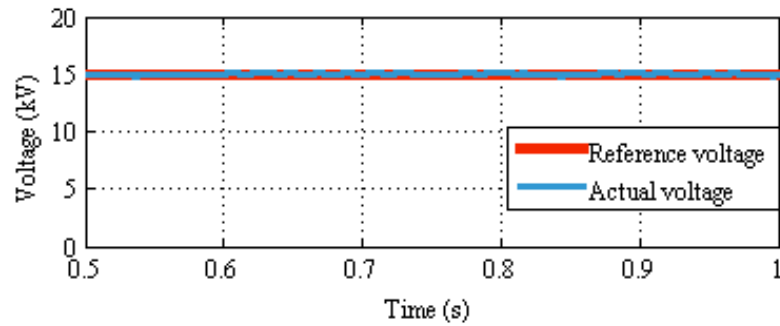


Figure 6.3: DC voltage across capacitor of APF inverter

As presented in Figs. 6.3, the APF controller worked as required, tracking both the voltage and current components well. For testing purposes, the data in table 7 is implemented with the LCI drive system and the motor is set to run with a constant speed. The current response of the APF control scheme is presented in Figs. 6.4/6.5, where the reference and actual plots of the d-q current components are shown.

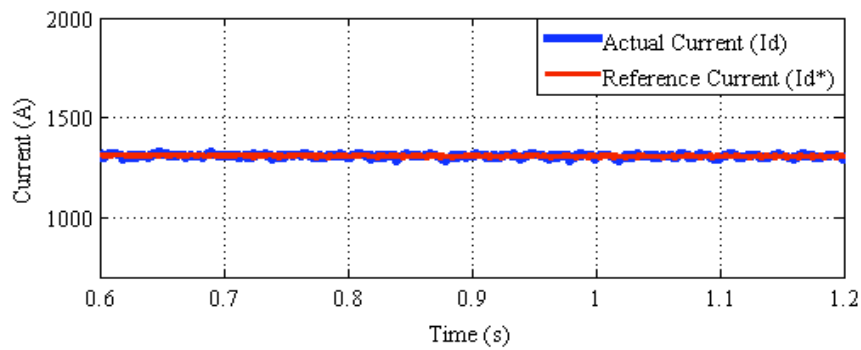


Figure 6.4: Id current component

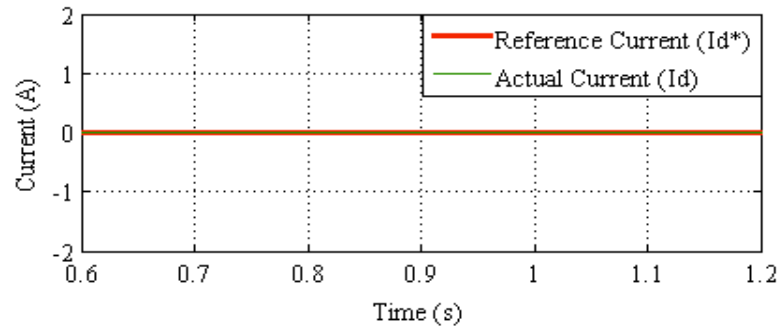


Figure 6.5: Iq current component

The grid currents are presented with and without the APF, alongside the respective THD components in Figs. 6.6-6.9.

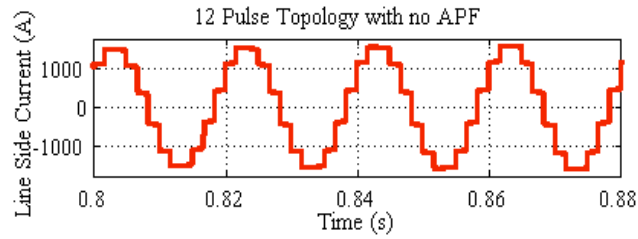


Figure 6.6: Grid current without APF

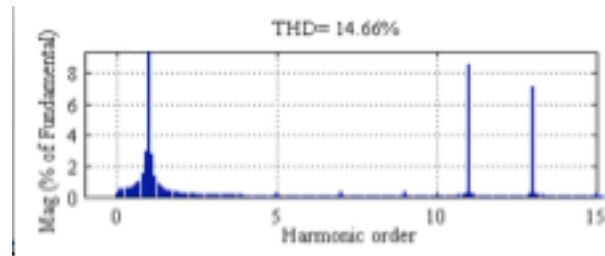


Figure 6.7: THD of current without APF

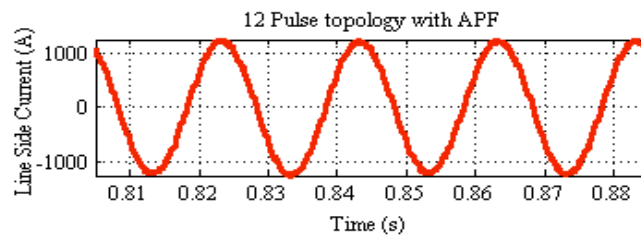


Figure 6.8: Grid current with tuned APF

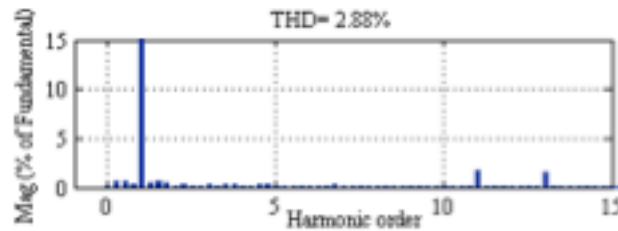


Figure 6.9: THD of current with APF

In general, the THD of the line/grid currents reduced by approximately 80% as presented in the Figs. 6.8-6.9. It is to be noted that this thesis presented both cases of active and passive filter implementations on the 12-pulse topology, and harmonics were reduced

greatly in both cases. The selection of one method over the other is primarily based on the client, where factors such as cost and performance have to be balanced.

6.3 APF FOR VAR COMPENSATION AND HARMONICS MITIGATION

As mentioned earlier, generally the operating firing angle of the rectifier block is around 30-40 degrees. This means that there is a reactive power in the system that might need compensation in order to achieve desirable power factor. This section provides the results obtained by using a PI current controller for the APF [74] for harmonic reduction and VAR compensation. The illustration in Fig. 6.10 presents this technique:

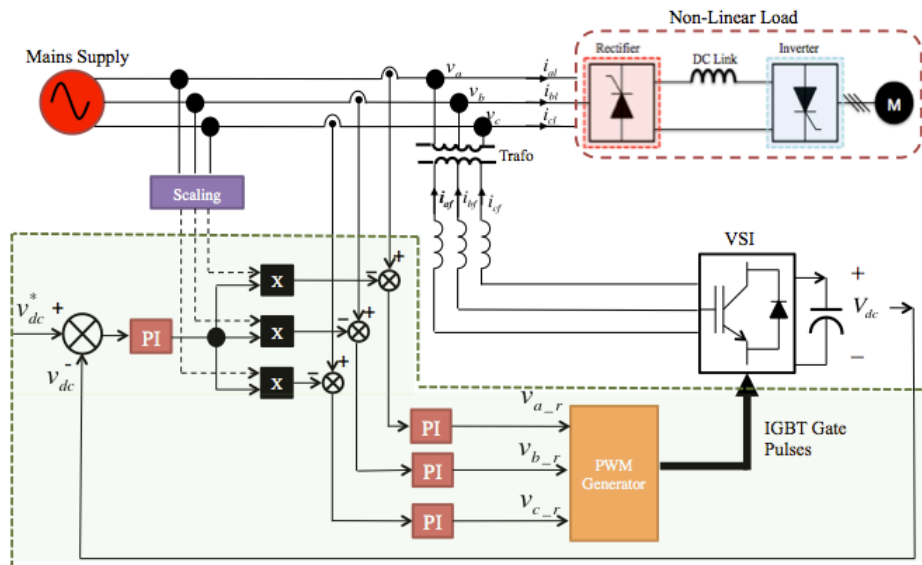


Figure 6.10: PI current control of APF

It is to be noted that the results presented next are at a high firing angle; therefore there is a large presence of reactive power in the system and its consequent compensation using the APF shown in figures presented. The plots from the simulation are presented as follows:

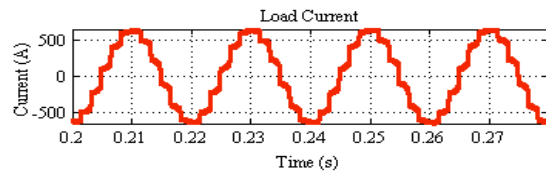


Figure 6.11: Load current

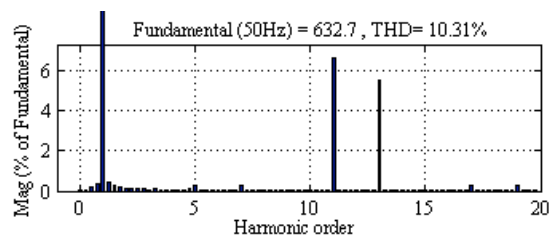


Figure 6.12: Harmonic content in the load current

In this technique the supply current is obtained by subtracting the filter current from the load current. The filter current and harmonic content is presented in Fig. 72/73.

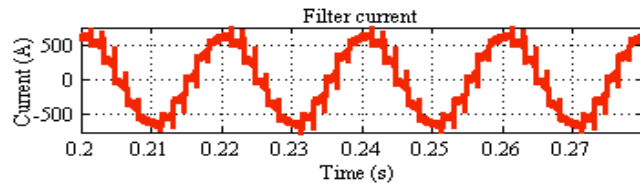


Figure 6.13: Filter current

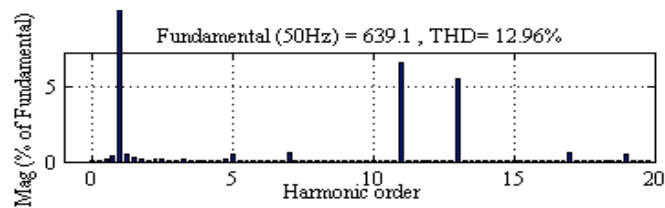


Figure 6.14: Harmonic spectrum

From Fig. 6.13, it is seen that the filter current is in quadrature to the supply current (Fig. 6.11) as and this signifies the compensation of reactive power in the supply currents. Following figures illustrate the supply voltage and current in phase with each other and consequently an ideal unity power factor.

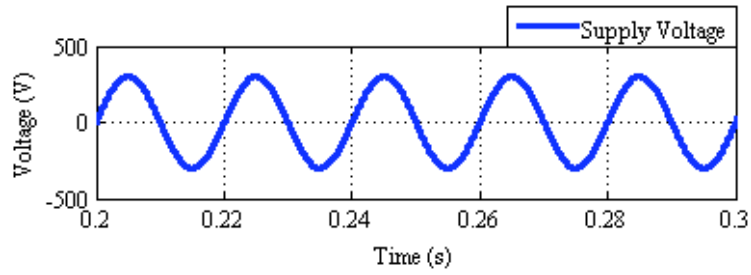


Figure 6.15: Supply voltage alongside current

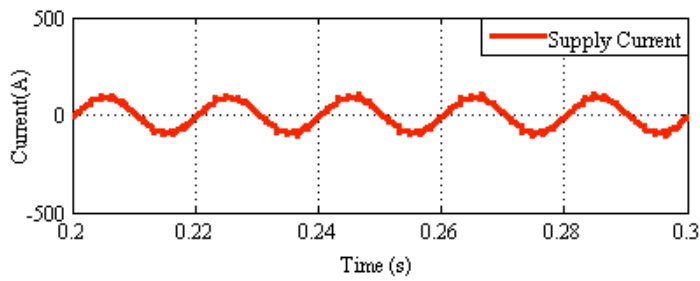


Figure 6.16: Filtered Supply Current

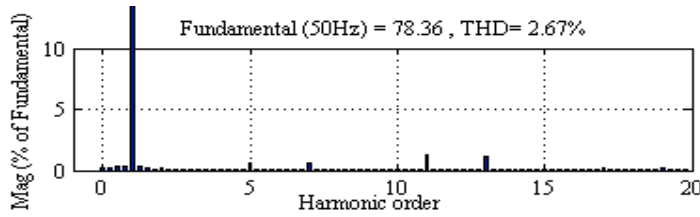


Figure 6.17: Frequency spectrum of supply current

Fig. 6.16 illustrates the spikes in the current waveform in order to see the impact of ideal “steps” of the converter topology, which isn’t present in practical cases. The presented results show reactive power compensation alongside harmonics mitigation.

6.4 DUAL FUNCTIONALITY OF THE VSI

The previous section presented the addition of an APF to the LCI drive system for harmonic mitigation and power factor improvement. Since, an external VSI is already being used as a starter for the presented drive; it can also function as an APF once the drive has started successfully. Fig. 6.18 illustrates the basic configuration of allowing both starting and filtering of harmonics using the same VSI.

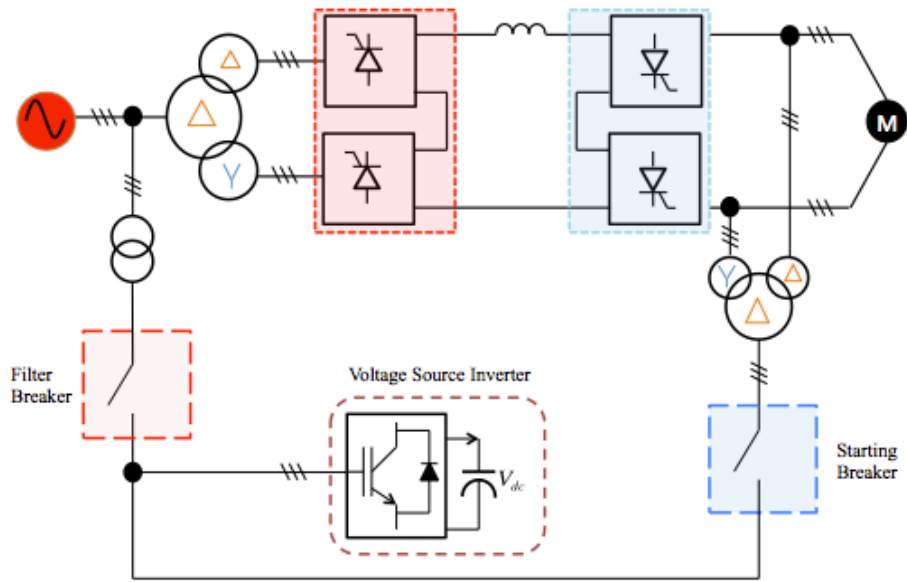


Figure 6.18: Dual function VSI

Initially, the starting breaker is closed and the filter breaker is opened. However when the drive starts operating the starting breaker is opened while the filter breaker is moved to closed condition. It should be noted that both the breakers are not to be in the closed state at the same time, therefore an interlock prevents this from happening.

CHAPTER 7 . CONCLUSION AND FUTURE WORK

The primary motivation of this thesis is to build a simulation model for the LCI drive and propose solutions and improvements regarding some of the encountered issues and problems mentioned earlier in the problem statement. Majority of the issues faced in practice deal with current harmonics being injected to the grid by the drive/load. To counter such problems, measures such as implementation of dual-secondary transformers are demonstrated in contrast to a conventional single secondary winding transformer. Higher pulse orders for the converters are also presented alongside a section dedicated to the implementation of passive and eventually active power filters, leading to improvements in THD of grid side currents.

Regarding the starting up of the LCC drive, an external VSI drive is put in place to allow easy start-up of the LCC drive. This VSI is further incorporated with an APF to provide the benefits of a starter as well as a harmonic filter.

The LCC drive model simulation design shows adequate speed and torque responses, matching actual operational conditions. The harmonics issues are dealt with multi-winding transformer and a 12-pulse converter topology. Instead of having a separately excited motor, a PMSM is used in this thesis, so issues with excitation currents, rotating diodes failures are not dealt with.

1. LCC drive model with speed control

The LCC model simulated in this thesis demonstrates a level of control and operation that is coherent with the actual drives used in this application. The

primary goal of the control is to maintain a steady speed while the torque fluctuates, and this was presented in the results accordingly.

2. Topologies for THD reduction

The topology implemented in this thesis is a 12-pulse topology. However, this thesis presented the advantages of this topology over a 6-pulse topology, as well as the possibilities of having 18, and 24 pulse topologies. The results are presented in terms of harmonic reductions and overall control response.

3. Active power filter implementation

Harmonics reduction is one of the most important factors related to the implementation of VFDs or LCC drives to be specific. Several THD reduction measure such as multi-winding transformers, multi-phase topologies are covered in point 1 and 2 as mentioned above. Apart from presenting the use of passive filters, active filters are implemented on the LCC drive topology to obtain reduced harmonics in the grid side and account for a major contribution to this thesis.

4. Dual functionality VSI

Finally, the external starter for the LCI drive is merged with the APF introduced in the later part of this thesis, enabling it to serve the function of a starter as well as a filter for the drive system.

FUTURE WORK

From the results presented in this thesis, a complete LCC drive has been modeled with the control system to study the topology further and propose solutions for the identified problems. Nonetheless, addressing all the identified problems in a Master thesis would be

difficult. Studying different starting techniques and implementing different motors such as separately excited type are considered as two main points to be addressed thoroughly. APF for high power applications can be further investigated in order to achieve better harmonic reduction and power factor correction.

Such drives are quite widely used in high power application and the points mentioned here can lead to major operational improvements if applied in practice.

REFERENCES

- [1] RasGas Company Limited. <http://www.rasgas.com>, (Accessed on 20 Sep 2015)
- [2] Emery, R.; Eugene, J., "Harmonic losses in LCI fed synchronous motors," in Petroleum and Chemical Industry Conference, 2001. IEEE Industry Applications Society 48th Annual, vol., no., pp.289-295, 2001
- [3] De Rosa, F.; Langella, Roberto; Sollazzo, A.; Testa, Alfredo, "On the interharmonic components generated by adjustable speed drives," in Power Delivery, IEEE Transactions on , vol.20, no.4, pp.2535-2543, Oct. 2005.
- [4] Carbone, Rosario; De Rosa, F.; Langella, Roberto; Testa, Alfredo, "A new approach for the computation of harmonics and interharmonics produced by line-commutated AC/DC/AC converters," in Power Delivery, IEEE Transactions on , vol.20, no.3, pp.2227-2234, July 2005.
- [5] Frank, W.-D., "Torque ripple considerations on large (mill) drives in the cement industry," in Cement Industry Technical Conference, 1995 IEEE, pp.411-432, 4-9 Jun 1995.
- [6] Mohamadian, S.; Tessarolo, A.; Shoulaie, A., "Design of an efficient starting circuit for LCI-fed synchronous motor drives," in Power Electronics, Drive Systems and Technologies Conference (PEDSTC), 2014 5th , vol., no., pp.31-36, 5-6 Feb. 2014
- [7] A. K. Jain and V. T. Ranganathan, "Starting scheme for load commutated inverter-fed wound field synchronous machine using an auxiliary low-power

- voltage source inverter," in IET Electric Power Applications, vol. 5, no. 6, pp. 494-502, July 2011.
- [8] A. K. Jain and V. T. Ranganathan, "Hybrid LCI/VSI Power Circuit—A Universal High-Power Converter Solution for Wound Field Synchronous Motor Drives," in IEEE Transactions on Industrial Electronics, vol. 58, no. 9, pp. 4057-4068, Sept. 2011.
- [9] S. D. Sudhoff, E. L. Zivi and T. D. Collins, "Start up performance of load-commutated inverter fed synchronous machine drives," in IEEE Transactions on Energy Conversion, vol. 10, no. 2, pp. 268-274, Jun 1995.
- [10] Hamad, M.S.; Abdelsalam, A.K.; Williams, B.W., "Over-voltage protection of single phase grid connected current source inverters using a simplified passive network," in Renewable Power Generation (RPG 2011), IET Conference on , vol., no., pp.1-5, 6-8 Sept. 2011
- [11] Jen-Nan Sheen, "Economic Feasibility of Variable Frequency Driving Pump by Fuzzy Financial Model," in Innovative Computing, Information and Control (ICICIC), 2009 Fourth International Conference on , vol., no., pp.934-937, 7-9 Dec. 2009
- [12] Inkyu Lee; Kyungjae Tak; Wonsub Lim; Il Moon; Kwang-Ho Choi, "Optimization of driver selection for minimizing cost on LNG plant considering risk factor," in Control, Automation and Systems (ICCAS), 2012 12th International Conference on , vol., no., pp.2222-2225, 17-21 Oct. 2012

- [13] Shakweh, Yahya, "Drives Types and Specifications", Chapter 32, Power Electronics Handbook: Devices, Circuits and Applications, Second Edition
- [14] K. Deacon, S. Lanier, J. Kubik and M. Harshman, "Managing technology step-outs and optimising process performance of starter-helper-generator VFDs on gas-turbine driven LNG trains," Petroleum and Chemical Industry Conference Europe, 2014, Amsterdam, 2014, pp. 1-9.
- [15] C. Wensheng, "Natural Gas Liquefaction Process for Small-scale LNG Project," Computer Distributed Control and Intelligent Environmental Monitoring (CDCIEM), 2012 International Conference on, Hunan, 2012, pp. 439-442.
- [16] Neidhofer, G.J.; Troedson, A.G., "Large converter-fed synchronous motors for high speeds and adjustable speed operation: design features and experience," in Energy Conversion, IEEE Transactions on , vol.14, no.3, pp.633-636, Sep 1999.
- [17] Plunkett, Allan B.; Turnbull, Fred G., "Load-Commutated Inverter/Synchronous Motor Drive Without a Shaft Position Sensor," in Industry Applications, IEEE Transactions on , vol.IA-15, no.1, pp.63-71, Jan. 1979.
- [18] Alcaso, A.N.; Cardoso, A.J.M., "Remedial Operating Strategies for a 12-Pulse LCI Drive System," in Industrial Electronics, IEEE Transactions on , vol.55, no.5, pp.2133-2139, May 2008.
- [19] Shakweh, Yahya, "Drives Types and Specifications", Ch. 33.1.4

- [20] Singh, B.; Singh, S.; Hemanth Chender, S.P., "Harmonics Mitigation in LCI-Fed Synchronous Motor Drives," in Energy Conversion, IEEE Transactions on , vol.25, no.2, pp.369-380, June 2010
- [21] Emery, R.; Eugene, J., "Harmonic losses in LCI fed synchronous motors," in Petroleum and Chemical Industry Conference, 2001. IEEE Industry Applications Society 48th Annual , vol., no., pp.289-295, 2001
- [22] Villablanca, M.E.; Nadal, J.I.; Cruzat, F.A.; Rojas, W.C., "Harmonic improvement in 12-pulse series-connected line-commutated rectifiers," in Power Electronics, IET , vol.2, no.4, pp.466-473, July 2009
- [23] TMEIC Corporation. "Variable Frequency Drives - a Comparison of VSI versus LCI Systems".
<https://www.tmeic.com/Repository/Media/Comparison%20of%20VSI%20versus%20LCI%20Systems%20FINAL.pdf>
- [24] Daryabak, M.; Filizadeh, S., "Analysis of waveform approximation for the AC current of a line-commutated converter," in Electric Power and Energy Conversion Systems (EPECS), 2013 3rd International Conference on , vol., no., pp.1-5, 2-4 Oct. 2013
- [25] Sudhoff, S.D., "Analysis and average-value modeling of dual line-commutated converter-6-phase synchronous machine systems," in Energy Conversion, IEEE Transactions on , vol.8, no.3, pp.411-417, Sep 1993

- [26] Jos Arrillaga, Yonghe H. Liu, Neville R. Watson, Nicholas J. Murray, "Self-Commutating Converters for High Power Applications", ISBN: 978-0-470-74682-0, October 2009
- [27] IEEE Guide for Self-Commutated Converters," in ANSI/IEEE Std 936-1987, 1987
- [28] T. Nakajima et al., "Multiple space vector control for self-commutated power converters," in IEEE Transactions on Power Delivery, vol. 13, no. 4, pp. 1418-1424, Oct 1998.
- [29] K. Sakamoto, M. Yajima, T. Ishikawa, S. Sugimoto, T. Sato and H. Abe, "Development of a control system for a high-performance self-commutated AC/DC converter," in IEEE Transactions on Power Delivery, vol. 13, no. 1, pp. 225-232, Jan 1998.
- [30] Hu, Y.; McKenzie, H.; Zhe Chen, "Voltage source converters in distributed generation systems," in Electric Utility Deregulation and Restructuring and Power Technologies, 2008. DRPT 2008. Third International Conference on , vol., no., pp.2775-2780, 6-9 April 2008
- [31] Bueno, E.J.; Garcia, R.; Marron, M.; Urena, J.; Espinosa, F., "Modulation techniques comparison for three levels VSI converters," in IECON 02 [Industrial Electronics Society, IEEE 2002 28th Annual Conference of the] , vol.2, no., pp.908-913 vol.2, 5-8 Nov. 2002
- [32] J. S. Lai and F. Z. Peng, "Multilevel converters—A new breed of power converters," IEEE Trans. Ind. Appl., vol. 32, no. 3, pp. 509–517, May/Jun. 1996.

- [33] M. Narimani, V. Yaramasu, Bin Wu, N. Zargari, G. Cheng and G. Moschopoulos, "A simple method for capacitor voltages balancing of diode-clamped multilevel converters using space vector modulation," Industrial Electronics Society, IECON 2013 - 39th Annual Conference of the IEEE, Vienna, 2013, pp. 310-315.
- [34] S. H. Hosseini and M. Sadeghi, "Reduced Diode Clamped Multilevel Converter with a modified control method," Electrical and Electronics Engineering (ELECO), 2011 7th International Conference on, Bursa, 2011, pp. I-302-I-306.
- [35] Petzoldt, J.; Delfo, S.; Jacobs, H.; Reimann, T., "Performance comparison of conventional two-level PWM-VSI and four-level flying capacitor PWM-VSI," in Industry Applications Conference, 2002. 37th IAS Annual Meeting. Conference Record of the , vol.1, no., pp.515-522 vol.1, 13-18 Oct. 2002
- [36] F. Filho, L. Tolbert and B. Ozpineci, "Multilevel cascade h-bridge inverter dc voltage estimation through output voltage sensing," Energy Conversion Congress and Exposition (ECCE), 2011 IEEE, Phoenix, AZ, 2011, pp. 185-189.
- [37] Antar, R.K.; Saied, B.M.; Khalil, R.A., "Using seven-level cascade H-bridge inverter with HVDC system to improve power quality," in Engineering Sciences (FNCES), 2012 First National Conference for , vol., no., pp.1-7, 7-8 Nov. 2012
- [38] Brovanov, S.V.; Egorov, S.D.; Dubkov, I.S., "Study on the efficiency at h-bridge cascaded VSI for different PWM methods," in Micro/Nanotechnologies and Electron Devices (EDM), 2014 15th International Conference of Young Specialists on , vol., no., pp.440-443, June 30 2014-July 4 2014

- [39] Bhattacharya, S.; Mascarella, D.; Joós, G., "Modular multilevel inverter: A study for automotive applications," in *Electrical and Computer Engineering (CCECE)*, 2013 26th Annual IEEE Canadian Conference on , vol., no., pp.1-6, 5-8 May 2013
- [40] B. Wu, J. Pontt, J. Rodriguez, S. Bernet and S. Kouro, "Current-Source Converter and Cycloconverter Topologies for Industrial Medium-Voltage Drives," in *IEEE Transactions on Industrial Electronics*, vol. 55, no. 7, pp. 2786-2797, July 2008.
- [41] K. Oguchi, H. Hama, and T. Kubota, "Multilevel current-source and voltage-source converter systems coupled with harmonic canceling reactors," in *32nd Annu. IEEE Industry Applications Conf. (IAS '97)*, vol. 2, 1997, pp. 1300–1308.
- [42] S. Kwak and T. Kim, "An Integrated Current Source Inverter With Reactive and Harmonic Power Compensators," in *IEEE Transactions on Power Electronics*, vol. 24, no. 2, pp. 348-357, Feb. 2009.
- [43] M. Hombu, S. Ueda, A. Ueda and Y. Matsuda, "A New Current Source GTO Inverter with Sinusoidal Output Voltage and Current," in *IEEE Transactions on Industry Applications*, vol. IA-21, no. 5, pp. 1192-1198, Sept. 1985.
- [44] S. Daher, R. Silva, and F. Antunes, "Multilevel current source inverter-The switching control strategy for high power application," in *Proc. 22nd Int. Industrial Electronics, Control, and Instrumentation Conf. (IEEE IECON)* , vol. 3, 1996, pp. 1752–1757.
- [45] Monteiro, V.; Exposto, B.; Pinto, J.G.; Sepulveda, M.J.; Nogueiras Melendez, A.A.; Afonso, J.L., "Three-phase three-level current-source converter for EVs fast

- battery charging systems," in Industrial Technology (ICIT), 2015 IEEE International Conference on , vol., no., pp.1401-1406, 17-19 March 2015
- [46] Azmi, S.A.; Ahmed, K.H.; Finney, S.J.; Williams, B.W., "Comparative analysis between voltage and current source inverters in grid-connected application," in Renewable Power Generation (RPG 2011), IET Conference on , vol., no., pp.1-6, 6-8 Sept. 2011
- [47] M. Beuermann, W. Fischer, P. Kalbfleisch, M. Hilscher and B. Blöcher, "Modular Load Commutated Inverters - A Proven Concept for High Power Applications," Industry Applications Society Annual Meeting, 2008. IAS '08. IEEE, Edmonton, Alta., 2008, pp. 1-7.
- [48] "Power semiconductors: For medium voltage Converters — An Overview," Power Electronics and Applications, 2009. EPE '09. 13th European Conference on, Barcelona, Spain, 2009, pp. 1-14.
- [49] Duffey, C.K.; Stratford, R.P., "Update of harmonic standard IEEE-519: IEEE recommended practices and requirements for harmonic control in electric power systems," in Industry Applications, IEEE Transactions on , vol.25, no.6, pp.1025-1034, Nov/Dec 1989
- [50] Sangshin Kwak; Toliyat, H.A., "A hybrid solution for load-commutated-inverter-fed induction motor drives," in Industry Applications, IEEE Transactions on , vol.41, no.1, pp.83-90, Jan.-Feb. 2005
- [51] Mital Patel , "Twelve pulse converter with differential delta connected transformer arrangement with reduced KVA capacities for line side harmonic

- reduction”, Electrical Department, Faculty of PG Studies & Research In Engineering & Technology Marwadi Education Foundation’s Group of Institutions Rajkot, India
- [52] Skibinski, G.L.; Guskov, N.; Dong Zhou, "Cost effective multi-pulse transformer solutions for harmonic mitigation in AC drives," in Industry Applications Conference, 2003. 38th IAS Annual Meeting. Conference Record of the , vol.3, no., pp.1488-1497 vol.3, 12-16 Oct. 2003
- [53] Malagon Carvajal, G.; Ordonez Plata, G.; Picon, W.G.; Chacon Velasco, J.C., "Investigation of phase shifting transformers in distribution systems for harmonics mitigation," in Power Systems Conference (PSC), 2014 Clemson University , vol., no., pp.1-5, 11-14 March 2014
- [54] Boudrias, J.-G., "Harmonic mitigation, power factor correction and energy saving with proper transformer and phase shifting techniques," in Electrical and Computer Engineering, 2004. Canadian Conference on , vol.1, no., pp.133-136 Vol.1, 2-5 May 2004
- [55] Jain, A.K.; Ranganathan, V.T., "Hybrid LCI/VSI Power Circuit—A Universal High-Power Converter Solution for Wound Field Synchronous Motor Drives," Industrial Electronics, IEEE Transactions on , vol.58, no.9, pp.4057,4068, Sept. 2011
- [56] P. Pejovic and D. Shmilovitz, "Low-harmonic thyristor rectifiers applying current injection," in *IEEE Transactions on Aerospace and Electronic Systems*, vol. 39, no. 4, pp. 1365-1374, Oct. 2003.

- [57] Vedam Subrahmanyam, "Thyristor Control of Electric Drives", Tata McGraw Hill Publishing Company Ltd. Page 119
- [58] N. R. Zargari, Yuan Xiao and Bin Wu, "A multi-level thyristor rectifier with improved power factor," *Industry Applications Conference, 1996. Thirty-First IAS Annual Meeting, IAS '96., Conference Record of the 1996 IEEE*, San Diego, CA, 1996, pp. 967-972 vol.2.
- [59] Hyung-Soo Mok; Seung-Ki Sul; Park, M.-H., "A load commutated inverter-fed induction motor drive system using a novel DC-side commutation circuit," in *Industry Applications*, IEEE Transactions on, vol.30, no.3, pp.736-745, May/Jun 1994
- [60] Tessarolo, A.; Castellan, S.; Menis, R., "Feasibility and performance analysis of a high power drive based on four synchro-converters supplying a twelve-phase synchronous motor," in *Power Electronics Specialists Conference, 2008. PESC 2008. IEEE*, vol., no., pp.2352-2357, 15-19 June 2008
- [61] Megadrive LCI. "Large adjustable-speed synchronous motor drives". http://www.vfservis.cz/files/001427_lci_brochure.pdf
- [62] Mohan, Undeland, and Robbins. *Power Electronics: Converters, Applications, And Design*. Third Edition. John Wiley and Sons Inc.
- [63] Chen, Bo-shi, "Automatic control system of electric power drive (3th edition)". Beijing, Mechanical industry press,2003.
- [64] Sobezuk D.L.; Rolak M.; "Modelling and Control of PWM Fed 6-phase Permanent Magnet Synchronous Machine", Warsaw University of Technology

- [65] Daoud, M.I.; Abdel-khalik, A.S.; Massoud, A.; Ahmed, S., "An asymmetrical six phase induction machine for flywheel energy storage drive systems," in *Electrical Machines (ICEM), 2014 International Conference on*, vol., no., pp.692-698, 2-5 Sept. 2014
- [66] E. Levi, R. Bojoi, F. Profumo, H. A. Toliyat and S. Williamson, "Multiphase induction motor drives - a technology status review," in *IET Electric Power Applications*, vol. 1, no. 4, pp. 489-516, July 2007.
- [67] Wang, B.; Wei, G. ; Chu, J.; Yi, G., "A novel modeling for a dual three-phase permanent magnet synchronous machine," in *Control, Automation, Robotics and Vision, 2008. ICARCV 2008. 10th International Conference on*, vol., no., pp.1630-1634, 17-20 Dec. 2008
- [68] Tessarolo, A.; Castellán, S.; Menis, R., "Analysis and simulation of a novel Load-Commutated Inverter drive based on a symmetrical five-phase synchronous motor," in *Power Electronics and Applications, 2009. EPE '09. 13th European Conference on*, vol., no., pp.1-11, 8-10 Sept. 2009
- [69] Gupta, R.K.; Mohapatra, K.K.; Somani, A.; Mohan, N., "Direct-Matrix-Converter-Based Drive for a Three-Phase Open-End-Winding AC Machine With Advanced Features," in *Industrial Electronics, IEEE Transactions on*, vol.57, no.12, pp.4032-4042, Dec. 2010
- [70] Massoud, A.M.; Ahmed, S.; Abdel-Khalik, A. S.; "Active Power Filter", Chapter 17, *Power Electronics for Renewable Energy Systems, Transportation and Industrial Applications*

- [71] S. Singh and B. Singh, "Power quality improvement using optimized Passive Filter for 12-pulse rectifier-chopper in LCI fed synchronous motor drives," Information and Communication Technologies (WICT), 2011 World Congress on, Mumbai, 2011, pp. 1104-1111.
- [72] S. M. Peeran and C. W. P. Cascadden, "Application, design and specification of harmonic filters for variable frequency drives," Applied Power Electronics Conference and Exposition, 1994. APEC '94. Conference Proceedings 1994., Ninth Annual, Orlando, FL, 1994, pp. 909-916 vol.2.
- [73] Singh, B.; Singh, S.; Hemanth Chender, S.P., "Power quality improvement in load commutated inverter-fed synchronous motor drives," in Power Electronics, IET , vol.3, no.3, pp.411-428, May 2011
- [74] Massoud A.M.; Finney S.J.; Williams B.W.; "Predictive Current Control of a Shunt Active Power Filter", 35th Annual IEEE Power Electronics Specialists Conference, 2004
- [75] El-Habrouk, M., Darwish, M.K. & Mehta, P. (2000) Active Power Filters: a review. Electrical Power Applications, IEEE Proceedings, vol. 147(5), 403-413
- [76] Pinto, J.G.; Exposto, B.; Monteiro, V.; Monteiro, L.F.C.; Couto, C.; Afonso, J.L., "Comparison of current-source and voltage-source Shunt Active Power Filters for harmonic compensation and reactive power control," in IECON 2012 - 38th Annual Conference on IEEE Industrial Electronics Society , vol., no., pp.5161-5166, 25-28 Oct. 2012

- [77] Herrera, R.S. and Salmeron, P. (2009) Instantaneous reactive power theory: a reference in the nonlinear loads compensation. *IEEE Transactions on Industrial Electronics*, 56(6), 2015-2022.

APPENDIX A: LCC TOPOLOGIES

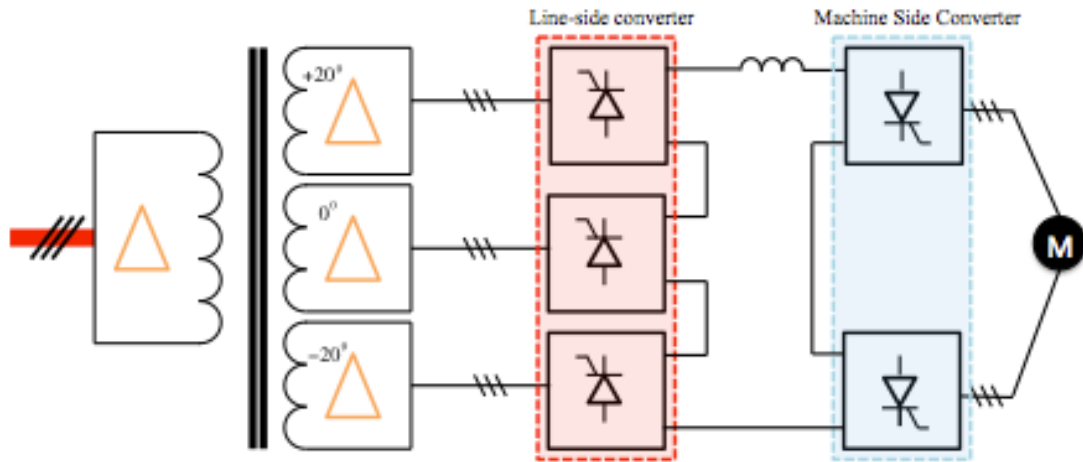


Figure AA.1: 18-pulse rectifier topology

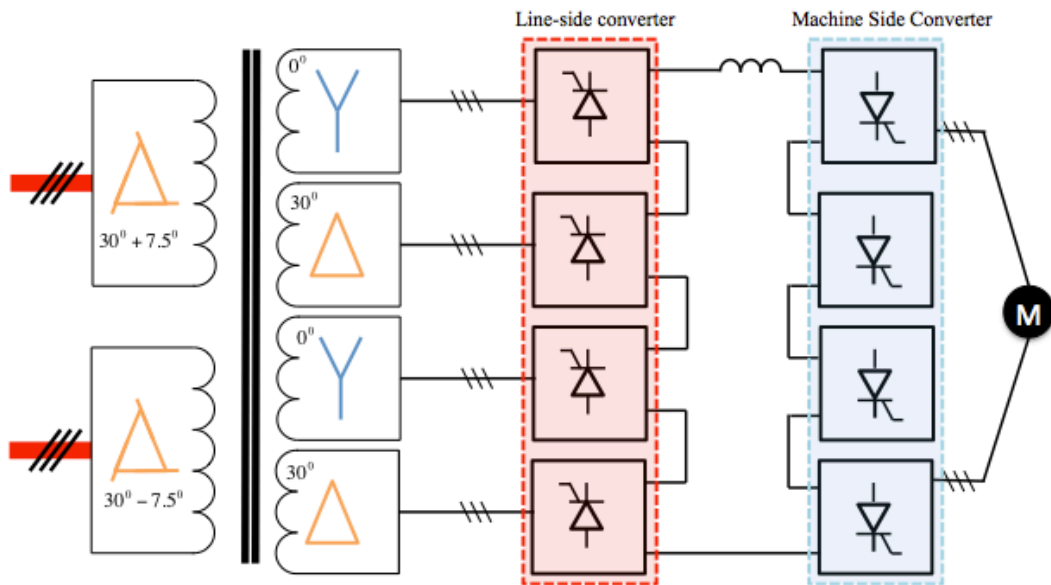


Figure AA.2: 24-pulse topology

APPENDIX B: THYRISTOR FIRING

A sample from the pulse-train of the thyristor firing sequence can be seen as shown in Fig. A.1 a relation between the frequencies of the firing pulses with the relative speed being tracked is also visible here.

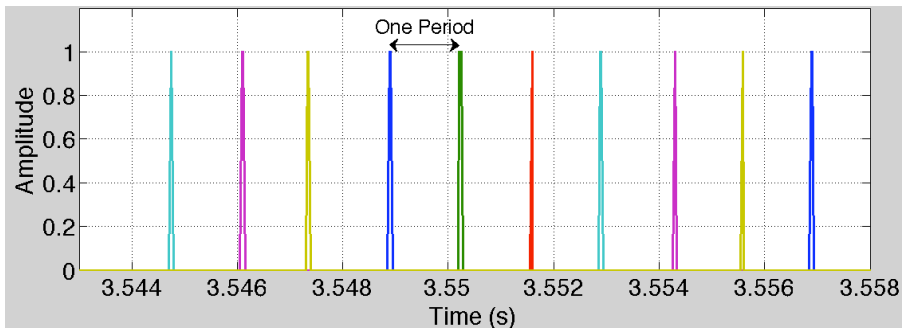


Figure AB.1: Thyristor Firing pulses at 800 rpm (period =0.001 s)

As shown in Fig. A.1 and A.2, as the speed reduces to almost half, the frequency of the fired pulses also reduces by half, providing justification for the operation of the pulse generator.

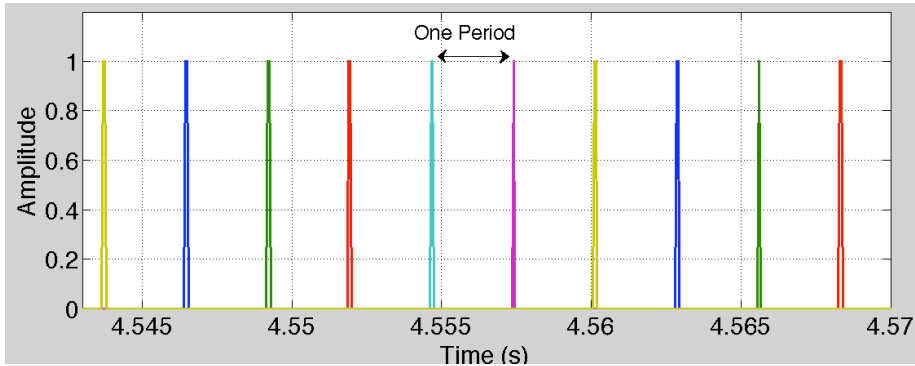


Figure AB.2: Thyristor firing pulses at 400 rpm (0.002 s)

APPENDIX C: LCC SIMULATION BLOCK

General Schematic

This figure shows the overall LCC drive system, with the line side converter, machine side converter in the 2x6 pulse configuration, the multi-phase transformers and the control loops for machine and line side thyristor angles.

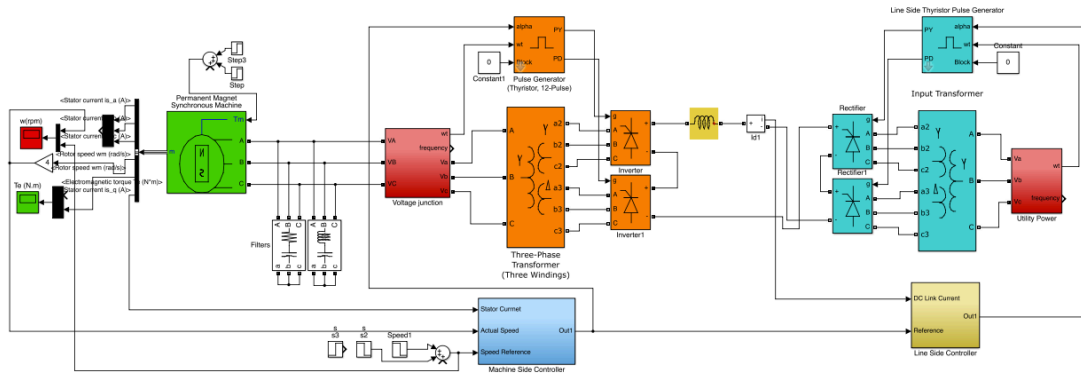


Figure AC.1: LCC Drive System Model in Simulink

LCC CONTROL

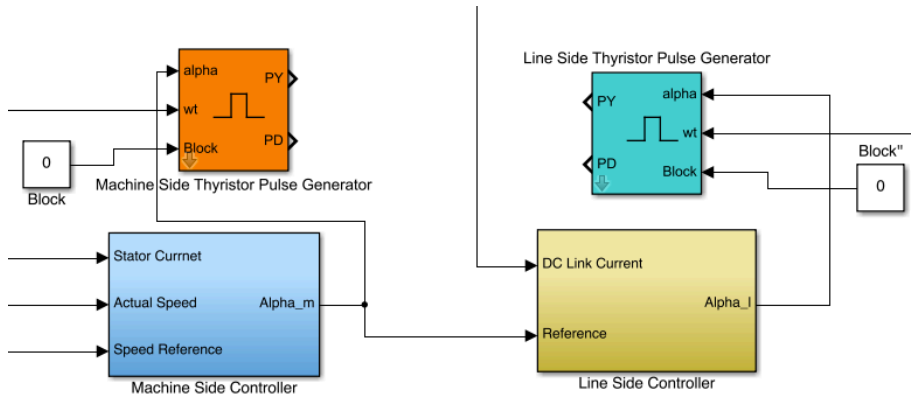


Figure AC.2: LCC Control Schematic

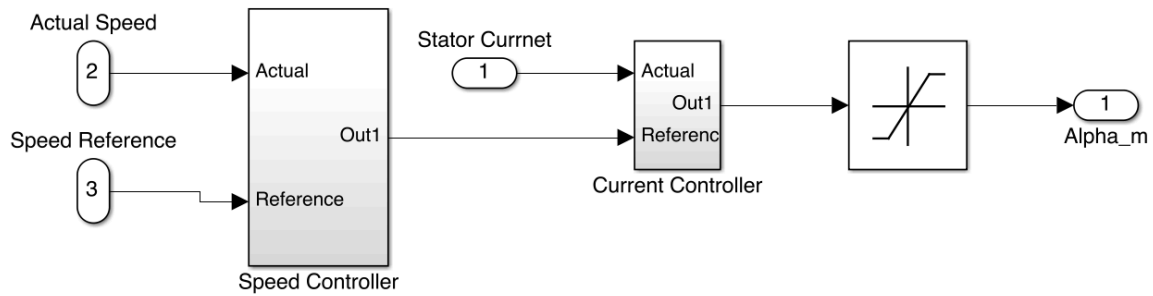


Figure AC.3: Speed and current control (Machine Side)

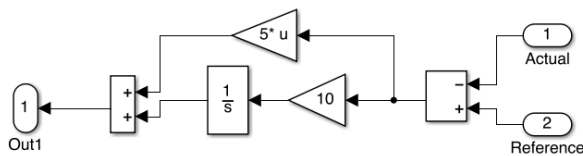


Figure AC.4: Under speed controller

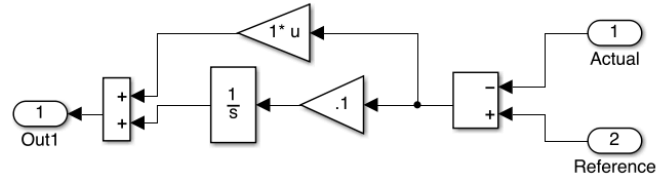


Figure AC.5: Under current control

Note: For the line side thyristor control, similar approach is used with the actual signal coming from the dc-link of the LCC.